HOLOCENE REEF ACCRETION: SOUTHWEST MOLOKAI, HAWAII, U.S.A.

MARY S. ENGELS,[1] CHARLES H. FLETCHER, III, [1] MICHAEL E. FIELD,[2] CURT D. STORLAZZI,[2] ERIC E. GROSSMAN,[2]
JOHN J.B. ROONEY,[1] CHRISTOPHER L. CONGER,[1] AND CRAIG GLENN[1]
[1] *Department of Geology and Geophysics, University of Hawaii, Honolulu, Hawaii 96822, U.S.A.*
e-mail: mengels@hawaii.edu
[2] *U.S. Geological Survey Pacific Science Center, University of California, Santa Cruz, California 95060, U.S.A.*

ABSTRACT: **Two reef systems off south Molokai, Hale O Lono and Hikauhi (separated by only 10 km), show strong and fundamental differences in modern ecosystem structure and Holocene accretion history that reflect the influence of wave-induced near-bed shear stresses on reef development in Hawaii. Both sites are exposed to similar impacts from south, Kona, and trade-wind swell. However, the Hale O Lono site is exposed to north swell and the Hikuahi site is not. As a result, the reef at Hale O Lono records no late Holocene net accretion while the reef at Hikauhi records consistent and robust accretion over late Holocene time.**

Analysis and dating of 24 cores from Hale O Lono and Hikauhi reveal the presence of five major lithofacies that reflect paleo-environmental conditions. In order of decreasing depositional energy they are: (1) coral–algal bindstone; (2) mixed skeletal rudstone; (3) massive coral framestone; (4) unconsolidated floatstone; and (5) branching coral framestone–bafflestone. At Hale O Lono, 10 cores document a backstepping reef ranging from ~ 8,100 cal yr BP (offshore) to ~ 4,800 cal yr BP (nearshore). A depauperate community of modern coral diminishes shoreward and seaward of ~ 15 m depth due to wave energy, disrupted recruitment activities, and physical abrasion. Evidence suggests a change from conditions conducive to accretion during the early Holocene to conditions detrimental to accretion in the late Holocene.

Reef structure at Hikauhi, reconstructed from 14 cores, reveals a thick, rapidly accreting and young reef (maximum age ~ 900 cal yr BP). Living coral cover on this reef increases seaward with distance from the reef crest but terminates at a depth of ~ 20 m where the reef ends in a large sand field. The primary limitation on vertical reef growth is accommodation space under wave base, not recruitment activities or energy conditions.

Interpretations of cored lithofacies suggest that modern reef growth on the southwest corner of Molokai, and by extension across Hawaii in general, is controlled by wave-induced near-bed shear stress related to refracted North Pacific swell. Holocene accretion patterns here also reflect the long-term influence of wave-induced near-bed shear stress from north swell during late Holocene time. This finding is consistent with other studies (e.g., Grigg 1998; Cabioch et al. 1999) that reflect the dominance of swell energy and sea level in controlling modern and late Holocene accretion elsewhere in Hawaii and across the Pacific and Indian oceans. Notably, however, this result is refined and clarified for Hawaii in the hypothesis of Rooney et al. (2003) stating that enhancement of the El Niño Southern Oscillation beginning approximately 5000 years ago led to increased north swell energy and signaled the end to net accretion along exposed coastlines in Hawaii. The exposure of Hale O Lono to north swell and the age of sea floor there (ca. 4,800 cal yr BP), coupled with the lack of north swell incidence at Hikauhi and the continuous accretion that has occurred there over the last millennium, strongly supports the ENSO reef hypothesis as outlined by Rooney et al. (2003). Other factors controlling Holocene reef accretion at the study site are relative sea-level position and rate of rise, and wave sheltering by Laau Point. Habitat suitable for reef accretion on the southwest shore of Molokai has shrunk throughout the Holocene.

INTRODUCTION

Holocene coral–algal reef accretion in the main Hawaiian Islands is described in detail by few studies, all from Oahu. Easton and Olson (1976) studied Hanauma Bay, Grigg (1998) studied Hanauma Bay, Mamala Bay, Kaneohe Bay, and Sunset Beach, and Grossman (2001) studied Kailua Bay. The data from these studies were used by Fletcher et al. (2001) to formulate an Oahu reef accretion model. The three major components of the Oahu reef system are an antecedent Pleistocene surface, a Holocene unit, and a thin veneer of modern coral growth that in places rests directly upon the Pleistocene surface.

The antecedent surface on Oahu is documented by Sherman et al. (1999) as ranging in age from marine isotope stage (MIS) 7 (ca. 200,000 cal yr BP) to late MIS 5c (ca. 97,000 cal yr BP) and MIS 5a (ca. 83,000 cal yr BP). According to the Oahu accretion model, Holocene reef accretion exploits the narrow region between wave base and the antecedent Pleistocene surface. Where wave limitations were absent, a late–middle Holocene (ca. 3,000 cal yr BP) sea-level highstand (+2 m) permitted maximum Holocene reef accretion and sediment production (Fletcher and Jones 1996; Grossman and Fletcher 1998). Fletcher et al. (2001) proposed that subsequent lower sea level in the late Holocene is responsible for a period of diminished reef development, and caused a seaward shift of accretion centers from the back-reef, reef crest, and upper fore-reef to the lower fore-reef slope. Their model also suggests that the greater part of Holocene accretion on Oahu is limited to areas of low wave energy where an antecedent Pleistocene foundation is absent, or at depths great enough to permit accretion below wave base (such as portions of Kailua Bay and Hanauma Bay). Additional accretion may also occur on the seaward edge of shelves or where deeper substrate has opened because of subaerial weathering during lower stands of the sea. The thin veneer of modern growth on Oahu overlies the combination of abundant Pleistocene and variable Holocene units (Jones 1993; Grigg 1998; Fletcher et al. 2001). The lack of modern reef development on Oahu results both from lack of accommodation space and high wave energy in the growth zone (Grigg 1998; Fletcher et al. 2001). On Oahu, environments suitable for reef accretion have diminished through time.

Rooney et al. (2003) summarize the findings of several drill-core studies of Holocene reefs around Kauai, Oahu, and Molokai. They reveal that in nearly all cases (subject to localized variations) fringing reef accretion proceeded apace through early Holocene time and ended at the start of the middle Holocene ca. 5000 years ago. They establish a relationship between the El Niño Southern Oscillation Index and winter-season storm occurrence in the North Pacific responsible for generating large damaging swell. Following their review of paleo-ENSO records from the Pacific basin, they hypothesize enhanced El Niño-related storm occurrence beginning ca. 5000 years ago and tie this to the end of net carbonate accretion by Hawaiian reef systems.

The fringing reef system defining the south shore of Molokai is the largest in the main Hawaiian Islands. Although there have been geologic studies of ancient land-based carbonate deposits on Molokai (Moore et al. 1994; Hearty et al. 2000) , there have been few studies of the geologic development of the fringing reef system. Study of the Molokai reef is important in order to establish comparisons to the Oahu system and thereby improve our understanding of Hawaiian reef development through time. Hawaiian reefs are an archive of environmental agents controlling carbon-

JOURNAL OF SEDIMENTARY RESEARCH, VOL. 74, NO. 2, MARCH, 2004, P. 255–269
 1527-1404/04/074-255/$03.00

ate accretion throughout the North Pacific that can be compared to archives elsewhere in the Pacific and Indian oceans.

In this paper we use subsurface cores and modern community surveys to study the geologic evolution of the reef at two sites, separated by only 10 km, situated on the southwestern corner of the island of Molokai. Benthic community data from this study and modeled wave-induced near-bed shear stress (WINBSS) from published data by Storlazzi et al. (2002) were used to establish a model for zonation of modern coral assemblages at each site. Radiocarbon dating of drill cores from each site allows for resolution of the temporal and lithologic history of the reef. Comparison of the modern assemblage model to the drill cores provides a basis for interpreting specific paleoreef environments (Cabioch et al. 1999). Study of paleoreef environmental patterns suggests that reef growth on the southwest corner of Molokai during Holocene time has been controlled by differences in WINBSS related to north swell, relative sea-level rise (RSLR), and wave sheltering by local geographic features.

Settings and Observational Data

Molokai, a high volcanic island in the Hawaii–Emperor chain, is 62 km (E–W) long and 13 km wide (N–S). Formed predominantly by two volcanoes, East Molokai (1.8 million years old) and West Molokai (1.9 million years old), Molokai is the fifth-largest island in the main Hawaiian Islands (Clague 1998). Created by the Hawaiian hotspot, Molokai is isolated from tectonic influences associated with continental and plate boundaries. Deformation of the lithosphere by volcanic loading at the hotspot, however, induces some vertical motion among the main islands (Jones 1993; Muhs and Szabo 1994; Grigg and Jones 1997; Rubin et al. 2000). However, no evidence has documented conclusively whether Molokai is stable, emerging, or submerging through time.

At roughly 21° N, 157° W, Molokai lies between Oahu and Maui and is protected on the south shore by the most extensive coral–algal fringing reef among the main Hawaiian Islands (Maragos 1998). This reef is 53 km in length and between 1 and 1.5 km wide, except near the ends of the island where the reef narrows, presumably because of high wave conditions. In general, the reef sustains a well-developed modern benthic community of carbonate accretors and bioeroders. The tidal range is 0.8 m with an average sea-surface temperature of 19° C and salinity of 35 ppt (Ogston et al. in press). The generalized cross-shore structure of the Molokai reef is typical for fringing reefs that have grown up to the position of sea level, consisting of a sand- or mud-dominated mangrove shoreline, a protected shallow reef flat landward of a high-energy reef crest (back-reef), spur-and-groove structures on the fore-reef slope, and a calm, deep-water sand field generally located in 20 m water depth or greater.

The back-reef has low coral cover, low coral diversity, and loading by muddy sediment from upland erosion. Water depth ranges from $<$ 1 m to $\sim$ 3 m with occasional vertical walled pits that mark the reef flat with relief of $\sim$ 10 m (Storlazzi et al. 2002). Landward portions of the back-reef are composed of a cobble-rich substrate with a prolific cover of turf algae (a multispecific assemblage of algae that traps ambient sediment and gradually encroaches on corals), dominated by terrigenous sediment loading. The seaward portion of the reef flat experiences improved circulation and water quality, though heavy sediment loading remains. Here the substrate is dominated by calcareous coralline algae (*Porolithon gardineri, Hydrolithon onkodes*), green algae (*Halimeda* sp.), and fleshy algae (*Sargassum* sp., *Dictyosphaeria* sp., *Turbinaria* sp., and *Dictyota* sp.) interspersed with occasional colonies of *Pocillopora damicornis, Pocillopora meandrina,* and *Porites lobata.*

Large coral heads increase in number at the reef crest, as does wave energy, while the terrigenous sediment load decreases. Water depth at the reef crest varies from $\sim$ 0.5 m at low-energy settings to $>$ 3 m where wave energy is higher. The fore-reef slope extends from the reef crest and ends at $>$ 20 m water depth in a large offshore sand field. At the reef crest and on the upper fore-reef slope the dominance of turf algae diminishes while coral coverage and diversity increase.

The morphology of the upper fore-reef slope consists of small scale spur-and-groove structures (relief of $\sim$ 1–2 m), while on the lower fore-reef slope the relief of the spur-and-groove structures increases to up to $>$ 3 m. The grooves may act as sediment traps, collecting echinoderm spines, *Halimeda* sp. flakes, sponge spicules, gastropod shells, terrigenous sediment, and fragments of corals and coralline algae. Major coral types in this region include *Montipora flabellata, Montipora capitata, Montipora patula, Pavona varians, Pocillopora meandrina, Porites compressa,* and *Porites lobata* which are interspersed and occasionally overgrown by the coralline algae *Porolithon gardineri* and *Hydrolithon onkodes.*

At greater depths near the foot of the fore-reef slope (15–20 m water depth) the diversity of coral decreases to nearly monospecific stands of delicately branching *Porites compressa.* At these depths the spur-and-groove morphology changes to low-lying reef promontories or islands (patches) extending into a large sand field that fronts much of the fringing reef on the south shore of Molokai.

The wave climate on Molokai is dominated by five types of ocean swell: north swell, trade-wind-generated waves, south swell, Kona storms, and hurricanes (Fig. 1). North swell, with periods of 14–20 s and wave heights ranging from 3 to 8 m (the mean annual maximum daily significant wave height is 7.8 m), and hurricane swell, with variable heights and periods, generate the largest and most destructive waves on the Hawaiian shoreline (Grigg 1998). The south shore of Molokai, in the lee of the island, is largely protected from north swell, which has dominant directions of 282°–45°, although refraction of north swell can have a significant impact on the east and west ends of the island. Tropical cyclones of hurricane strength occur infrequently in Hawaii, about once every 40 years (Dollar 1982; Dollar and Tribble 1993), and damage to coral reefs associated with hurricane swell varies with storm direction, intensity, and duration. Hurricane impacts on the south shore of Molokai depend on the storm track, which determines how much wave shadowing occurs from nearby islands.

Trade-wind-generated waves in Hawaii are normally from the northeast or east (0°–123°) with periods of 5–9 s and heights of 1–3 m, and persist 90% of the summer months and 55–65% of the winter months (Grigg 1998). The east–west orientation of Molokai blocks normal trade-wind approach along the south shore, but as trade winds impinge on the high remains of the East Molokai volcano the winds split into two paths. One half flows around the east end of Molokai and approaches parallel to the southern shore from the east. The other path flows westward along the northern coast and converges with the southern component through the low valley between the East and West Molokai volcanoes (Schroeder 1993). Trade-wind interaction with local island heating causes damping of the trade winds in the morning and evening when island cooling generates downslope breezes. But during the day, as the island heats, trade-wind activity is enhanced (Schroeder 1993). This Molokai ''vortex'' means that trade-wind-generated seas along the southern shore, including the southwest shore, come from the east, where there is no wave shadowing by other islands.

Low (1–2 m height), long-period (14–22 s), south swell (147°–210°) most commonly affects Hawaiian shorelines between April and September. These waves are generally considered to be beneficial to coral reefs in Hawaii, increasing circulation without causing significant damage (Grigg 1998). Wave shadowing by Lanai reduces the impact of southern swell from 147° to 180° on the south shore of Molokai.

Kona storm waves with periods between 6 and 12 s and significant wave heights up to 4 m approach from the southwest to southeast (147°–258°), and occasionally have detrimental impacts on Hawaiian reefs (Grigg 1998). Winds driving these swells are generated by local low-pressure fronts in the islands. From 147° to 180° the southern shore of Molokai is protected from these waves by the wave shadowing by Lanai.

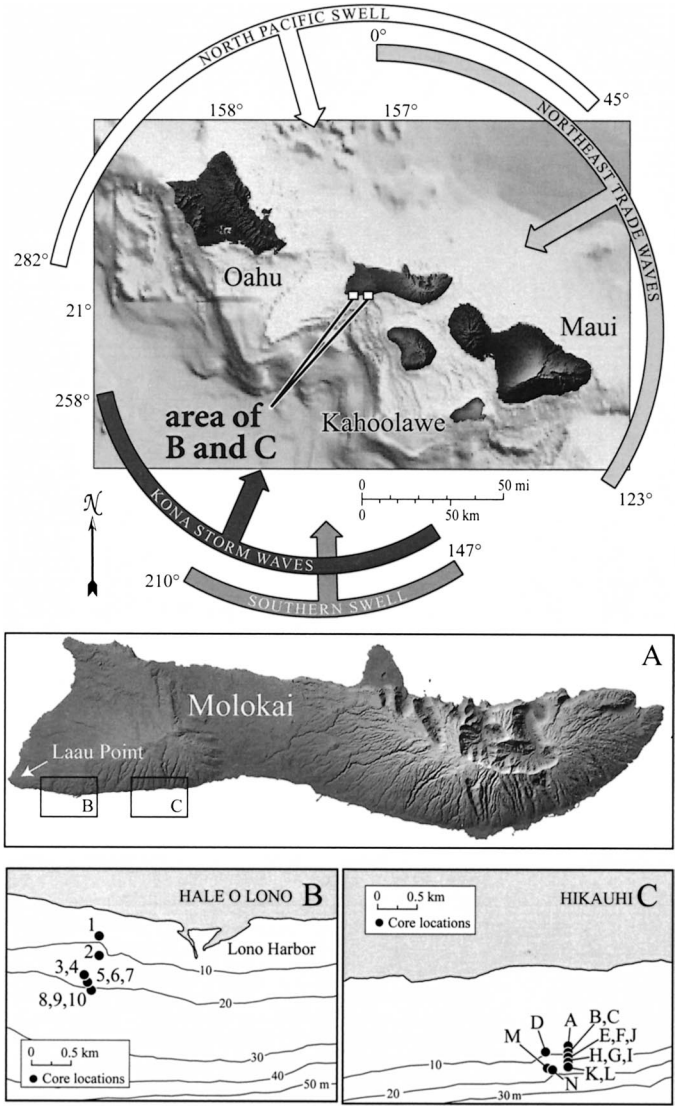

FIG. 1.—Study Site. Overview of Molokai showing dominant swell types and directions. The south shore of Molokai is most affected by south, Kona, and trade-wind waves, although the ends of the island experience impacts from refracted north swell. The southeastern shore of Molokai is partially protected from southern and Kona wave impacts by the island of Lanai. **A)** Location map showing drill sites on the southwestern corner of Molokai. **B)** All cores from Hale O Lono are labeled numerically, increasing in number with depth. **C)** Cores from Hikauhi are labeled alphabetically, advancing with depth.

Study Sites

This study focuses on two sites, Hale O Lono (HOL) at 21°5′ N, 157° 15′ W and Hikauhi 21°5′ N, 157°10′ W, both located at the southwestern end of the fringing reef and separated by 10 km (Fig. 2). The HOL site is characterized by poorly developed modern community veneer on middle Holocene fossil limestone. The site has a gradual depth gradient with sparse coral cover and shore-parallel ridge-and-runnel morphology of solid reefal limestones with interspersed narrow sand fields. In addition to south swell impact, easterly trade winds at 8–21 knots generate wind swell that affects this shoreline during summer months. During winter months this site experiences high-energy, refracted north swell with decreased trade-wind swell and possible Kona storm impacts. HOL may experience strong tidal currents because it lies adjacent to the Kaiwi Channel separating Oahu and Molokai. Sediment loading at HOL is small because of minimal run off from the arid to semiarid uplands, but suspension of carbonate sediment is significant during periods of high wave energy.

At Hikauhi, the depth gradient is gradual, coral cover is abundant, the reef displays shore typical, well-developed spur-and-groove morphology and there is a marked drop-off into a large sand bed at ~ 17 m with patch reefs consisting of monospecific stands of *Porites compressa* at greater depths. Fossil reef exposure is limited at this site. Summer swell impact on this site is the same as for HOL. In the winter, impact from refracted north swell is greatly diminished relative to HOL because of the distance (15 km) of this site from the western end of the island (Storlazzi et. al. 2002). While Hikauhi does not experience strong tidal currents, there is significantly more upland sediment loading at this site than at HOL. Stream gullies on adjacent watersheds have intermittent flow that is maximized during rain events. Inside the shallow reef crest a layer of fine brown sediment, likely a mixture of terrigenous muds and fine-grained carbonates, covers much of the benthic surface and is often bound by turf algae. The suspended carbonate sediment component here is less than at HOL, because this environment receives less wave energy.

METHODOLOGY

This study utilizes modern benthic community data and a suite of reef cores from each site to address the Holocene accretion history. Benthic community data were collected for analysis of modern community composition and to establish a model for zonation of modern coral assemblages. Structural components of drilled reef cores were compared to the modern zonation to determine a suite of lithofacies that best describe past depositional environments. Using the distribution of lithofacies within the cores and across the reef structure, we determined paleoenvironmental conditions and the progression of whole-reef accretion through time.

Benthic community data were collected using modified line-intercept techniques (LIT) in water depths from 4 m to 21 m after Montebon (1992). Surveys were conducted by laying a 10 m line along the benthic surface and recording the position of every change in substrate type. In addition to substrate changes, other parameters recorded for each site included: surface morphology; coral species, morphology, and associations; algal species, morphology, and associations; and presence of bioeroders and zoanthids. Approximately 20 surveys were collected at each site in both shore-normal and shore-parallel directions and across the entire reef structure to account for whole reef morphology. Species diversity and morphologic diversity were calculated after Harney (2000) using the Shannon–Weaver diversity index (1949) with the equation $Hc = -\text{sum}\,(p_i \times ln\ p_i)$ where Hc is diversity, p_i is the percent cover of the i^{th} species or morphologic form. Values < 0.5 indicate low diversity.

For drilling we employed a diver-operated, submersible, hydraulic, rotary, un-cased bit and rod, Tech 2000 drill system modified after Macintyre (1975). In our tests, this system yielded better recovery of core from unconsolidated reef than the cased wireline (NQ2) system distributed by Boart Longyear that we have also used. The bits are diamond-studded and 7.6 cm in diameter. We used drill pipe lengths of 40 cm, 76 cm, and 152 cm (internal lengths of 30 cm, 66 cm, and 142 cm respectively). A roughly shore-normal transect of cores was collected at each site in water depths ranging from 4 m to 21 m. Where possible, cores were started on a live surface to constrain the upper boundary of growth. Sample recovery ranged from 20% to 100% and averaged 69%. Average recovery for HOL (10 cores) was 80%, whereas cores from the Hikauhi site (14 cores), where the reef framework is unconsolidated and replete with loose sediment, had average recovery of 56%. We specifically targeted massive *Porites lobata* as a starting point for our cores to improve recovery at Hikauhi. This lead to an overrepresentation of this species in our cores relative to distribution in the modern environment.

All cores collected were halved and photographed for archiving. Limestones were classified according to the Embry and Klovan (1971) modifi-

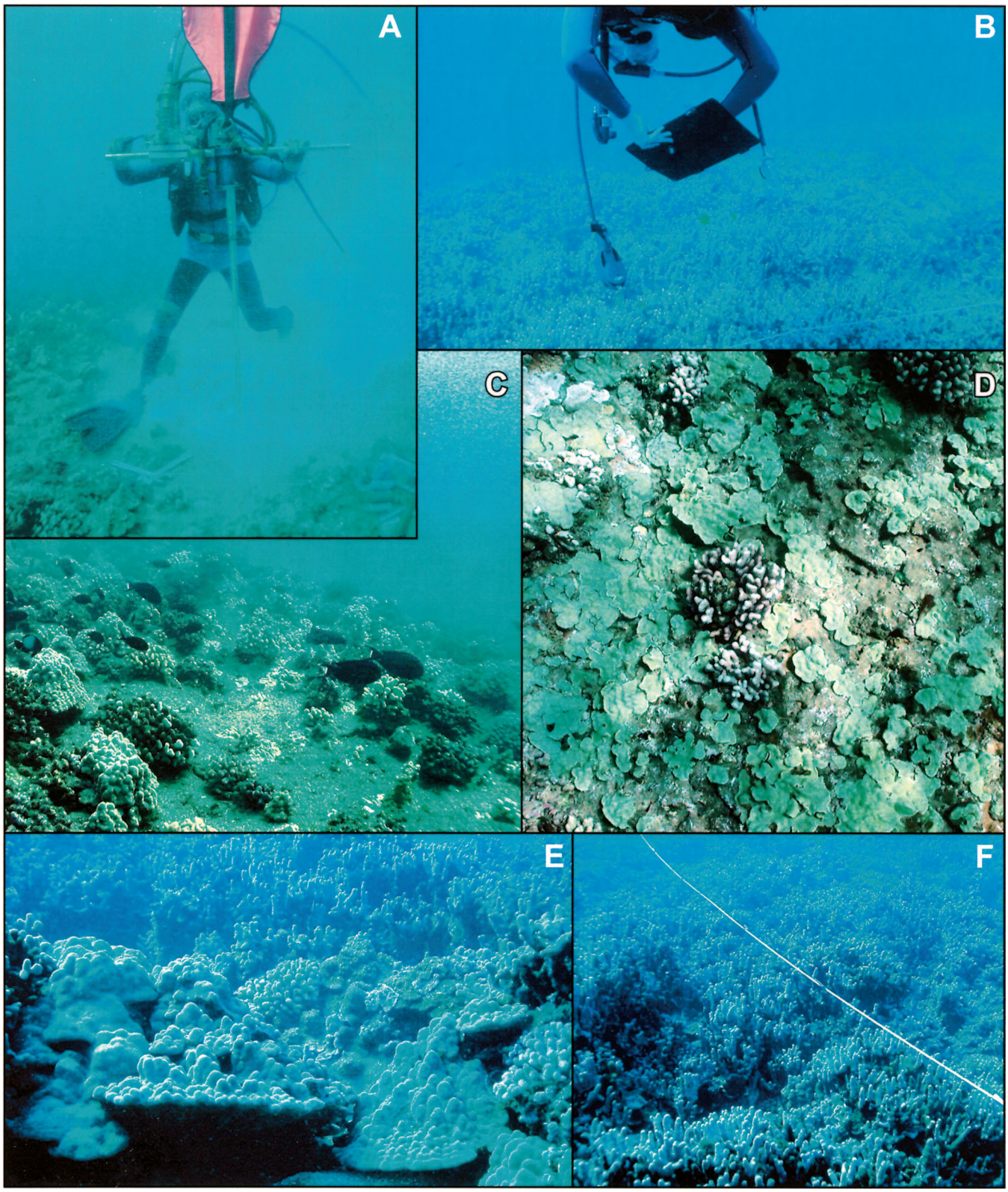

FIG. 2.—Coral Associations. **A)** Typical drilling operation at Hikauhi. **B)** Benthic surveys utilized the line-intercept technique after Montebon (1992). **C)** High-energy (> 10 m) community at Hale O Lono showing stout branching *Pocillopora meandrina* and massive *Porites lobata,* with abundant encrusting *Porites lobata* on middle Holocene age fossil reef substrate (ca. 4,800 cal yr BP). **D)** High-energy (< 5 m) community at Hale O Lono showing stout branching *Pocillopora meandrina* and encrusting *Montipora patula,* and *Montipora capitata* on middle Holocene age fossil reef substrate. **E)** Low-energy (5–10 m) community at Hikauhi showing stout-branching *Pocillopora meandrina,* massive *Porites lobata,* and finger-branching *Porites compressa.* **F)** Low-energy (> 10 m) community at Hikauhi showing nearly monospecific stand of finger-branching *Porites compressa.*

cation of the Dunham (1962) scheme. Cores were sampled for radiometric, petrographic, mineralogic, and geochemical analyses. Approximately 20 thin sections from both sites were analyzed petrographically to determine the degree of aragonite recrystallization and the extent and type of cementation. Core logs detail type and degree of lithification, transition horizons, presence and type of bioeroders, associated microflora and microfauna and any associated staining. Determinations of five dominant lithofacies were made following Grossman (2001). These lithofacies were used in conjunction with modern assemblage zonation to determine paleoreef environments (for validity of this methodology see Fairbanks (1989), Cortes et al. (1994), Montaggioni and Faure (1997), and Cabioch et al. (1999)).

Radiocarbon and X-ray diffraction (XRD) sample material was cleaned with deionized H_2O in an ultrasonic cleaner until water remained clear of debris. A 15% laboratory grade H_2O_2 bath was used to remove any remaining organic contamination. A second deionized H_2O ultrasonic bath followed by a 10% HCl acid etch and drying in a 38° C oven completed sample preparation. XRD analysis was performed at the Department of Geological Sciences, Southern Methodist University, with a Scintag (Thermo Optek) PAD V Powder diffraction system. The XRD was calibrated with a quartz standard, and the samples were scanned from two theta 25° to 31° in 0.2° increments. Aragonite percentages were calculated after Sabine (1992). The *d*-spacing offset of the calcite peak was used to determine mole percent of $MgCO_3$ in calcite phases after Bischoff et al. (1983).

Radiocarbon ages were obtained from the National Ocean Sciences Accelerator Mass Spectrometry (NOSAMS) facility at Woods Hole Oceanographic Institution. NOSAMS provided conventional radiocarbon age and 1 sigma error, including corrections for isotopic fractionation based on $\delta^{13}C$ values determined during AMS analysis. Radiocarbon ages were further calibrated to calendar years before present (cal yr BP) using Calib 4.12 (Stuiver and Reimer 1993) and the 1998 INTCAL Calibration data sets (Stuiver et al. 1998). A marine reservoir correction of 115 ± 50 years for regional Hawaiian marine waters was used after Stuiver and Braziunas (1993).

RESULTS

Modern Assemblage Zonation

Hale O Lono.—At HOL, a gently sloping mid-Holocene reef pavement is present just seaward of the shoreline and continues offshore to depths of 20 m or greater. Here the modern community, as determined from twenty-seven 10 m survey lines, can be divided into three somewhat overlapping assemblage zones delineated by water depth: < 5 m, 5 to 10 m, and > 10 m.

In the shallowest region (< 5 m) the exposed fossil reef pavement lacks spur-and-groove structures, experiences high wave energy, and is consistently scoured with sand and rubble. The reef pavement surface is smooth with intermittent turf algae and is incised by small shore-normal sand channels < 0.5 m in depth and width. The substrate in this area is dominated by fossil reef with low living coral cover characterized by low coral and morphological diversity (Table 1). The few established corals generally adopt encrusting growth morphology to minimize breakage, with the notable exception of *Pocillopora meandrina,* the dominant coral species, which maintains a stoutly branching form (Fig. 2). In this region we observe accretion of the reef structure occurring via encrustation by corals (*Montipora patula, Montipora capitata*) and coralline algae (branching *Porolithon gardineri,* encrusting *Hydrolithon onkodes*), producing a solidly cemented reef structure with little pore space. One unique form of potential reef accretion involves the coral *Pocillopora meandrina* and the coralline algae *Porolithon gardineri* and *Hydrolithon onkodes.* Once a *Pocillopora meandrina* colony has been established, *Porolithon gardineri* flourishes within the sheltered spaces between branches, growing upward until level with the tops of the *Pocillopora meandrina.* Thick layers of *Hydrolithon onkodes* grow over the top of both the *Pocillopora meandrina* and the *Porolithon gardineri,* encapsulating the entire coral colony and creating a flat surface upon which coral recruitment begins anew.

TABLE 1.—*Summary of data from benthic ecosystem survey.*

HALE O LONO		
<5 m	5 to 10 m	>10 m
Coralline algae cover as percent of total substrate:		
0–22% (average 21%)	0–20% (average 10%)	0–7% (average 1%)
Coral cover as percent of total substrate:		
6%–22% (average 15%)	18%–66% (average 41%)	1%–16% (average 8%)
Dominant coral types–% total substrate (% living coral cover normalized to 100)*		
M. capitata–2% (12%)	*M. capitata*–3% (7%)	*M. capitata*–0% (2%)**
M. patula–4% (25%)	*M. patula*–12% (30%)	*M. patula*–0% (4%)**
M. flabellata–0% (2%)**	*P. meandrina*–15% (38%)	*P. meandrina*–1% (4%)
P. meandrina–5% (35%)	*P. compressa*–1% (1%)	*P. lobata*–7% (90%)
P. lobata–4% (26%)	*P. lobata*–10% (24%)	
Dominant coral growth morphologies by depth zone:		
encrusting	encrusting	encrusting
stout branching	finger branching	massive
	massive	stout branching
	stout branching	
Coral species diversity by depth zone:		
0.45	0.77	0.22
Coral growth morphology diversity by depth zone:		
0.45	0.8	0.22
HIKAUHI		
<5 m	5 to 10 m	>10 m
Coralline algae cover as percent of total substrate:		
0–23% (average 14%)	0–22% (average 9%)	0–2% (average 1%)
Coral cover as percent of total substrate:		
26%–67% (average 52%)	52%–78% (average 68%)	60%–96% (average 86%)
Dominant coral types–% total substrate (% living coral cover normalized to 100)*		
M. capitata–6% (13%)	*M. capitata*–12% (20%)	*M. capitata*–24% (29%)
M. patula–12% (20%)	*M. patula*–25% (37%)	*M. patula*–6% (8%)
P. meandrina–14% (27%)	*P. meandrina*–2% (3%)	*P. meandrina*–3% (4%)
P. compressa–16% (32%)	*P. compressa*–21% (30%)	*P. compressa*–38% (43%)
P. lobata–4% (6%)	*P. lobata*–7% (9%)	*P. lobata*–15% (16%)
Dominant coral growth morphologies by depth zone:		
encrusting	encrusting	encrusting
finger branching	finger branching	finger branching
stout branching	massive	massive
Coral species diversity by depth zone:		
1.01	1.11	1.15
Coral growth morphology diversity by depth zone:		
1.02	1.13	1.16

* Abbreviated names, full name given below, ** values <1 reported as 0%.
Montipora capitata, Montipora flabellata, Montipora patula, Pocillopora meandrina, Porites compressa, Porites lobata

At intermediate depths, 5–10 m, live coral cover reaches its maximum for HOL (Table 1). Here the reef pavement displays increased rugosity (a paleokarst surface?) allowing the propagation of delicate coral species including thin columnar *Porites compressa* in highly localized protected sites. Wave energy remains high, and we infer that exposed reef pavement is mostly scoured clean of algal and coral growth. However, species and morphologic diversity peak in this area as corals utilize open substrate in the low-energy shadows created by relief of the reef pavement. Encrustation, similar to that occurring in the shallower regions, is the dominant morphologic form occurring here. Substrate voids are often infilled with rubble. These accumulations may then lithify or not. This rubble is often encrusted on all sides by *Hydrolithon onkodes,* likely from time spent shifting on the benthic surface prior to deposition.

At depths greater than 10 m, the reef pavement forms smooth shore-parallel bands alternating with sand fields with relief 0.5 m to 1 m below the surface of the reef pavement. The width of the reef pavement is greater at shallow depths but decreases with depth. Although this area is below wave base except for large waves, there is a very strong tidal current that

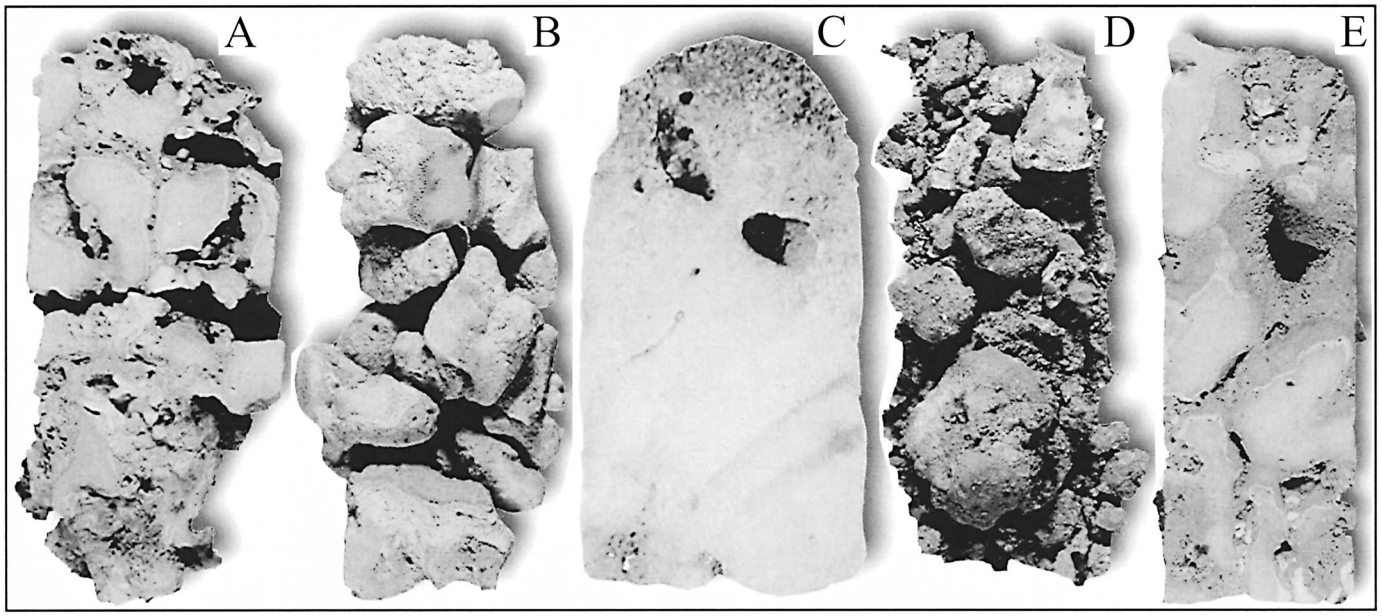

FIG. 3.—Lithofacies. In order of decreasing depositional energy: **A)** coral–algal bindstone, **B)** mixed skeletal rudstone, **C)** massive coral framestone, **D)** unconsolidated floatstone, **E)** branching coral framestone–bafflestone.

sweeps the reef pavement. On the pavement surface modern coral cover has very low relief (< 1 m) and is interspersed with turf algae. In general, coral colonies, dominated by massive and encrusting *Porites lobata,* are 15 cm in diameter or less and are sparse. In this depth zone, living coral cover, species diversity, and morphological diversity drop to the lowest values seen at HOL. Observationally, rubble accumulation is the likely mechanism for reef accretion at these depths. Encrusting coralline algae (*Porolithon gardineri* and *Hydrolithon onkodes*) are rare at these depths.

Hikauhi.—Hikauhi has a fringing reef structure with a backreef, reef crest, and fore-reef slope that terminates in a large offshore sand field at ~ 17 m depth. A total of 19 surveys from the reef crest across the fore-reef slope reveal three somewhat overlapping assemblage zones corresponding to water depths of < 5 m, 5 to 10 m, and > 10 m. We observe accretion taking place across the fore-reef slope as a mixture of encrustation and overgrowth by coral (*Montipora capitata,* and *Montipora patula*) and coralline algae (*Hydrolithon onkodes*), and burial of *in situ* colonies by accumulation of rubble and carbonate sediment. Encrusting accretion appears to be more prevalent in intermediate and shallow regions of the fore-reef slope whereas overgrowth and rubble accumulation occurs more often at greater depth.

In the shallow region (< 5 m), low-relief (< 1 m) spur-and-groove morphology is interspersed with large (100 m to 200 m in length) sand-floored dead-end channels with up to 4 m vertical relief (reentrants). Although spur-and-groove structures are oriented approximately normal to the dominant swell, the reentrants do not have a preferred orientation. The floors of grooves are a mixture of sand, small coral rubble, fine terrigenous sediment, and *Halimeda* sp. flakes, and the walls are covered with platy corals (*Porites* sp. and *Montipora* sp.). Living coral cover, species, and morphologic diversity are lowest in the shallow zone at Hikauhi (Table 1). The three most abundant coral species are (in decreasing order) *Porites compressa, Pocillopora meandrina,* and *Montipora patula. Porites compressa* and *Montipora patula* remain among the dominant corals at all depths, but abundance of *Pocillopora meandrina* diminishes rapidly with depth. The zoanthid *Palythoa tuberculosa* was observed only at Hikauhi, and only at shallow depths.

Spur-and-groove structures with up to 2 m of relief and oriented normal to the onshore swell direction typify the benthic morphology at 5–10 m water depths. The benthic substrate shows a marked increase in live coral cover (%), species diversity, and morphologic diversity relative to shallower locales. *Porites lobata* colonies in this region increase in size and adopt a massive growth morphology not seen in shallower waters. At these depths *Montipora patula* outcompetes *Porites compressa* by a small margin. With high coral density, a unique association forms with *Montipora* sp. growing in and around the branches of *Porites compressa,* encrusting lower regions of the columnar form.

The deepest region (> 10 m) encompasses a transition from spur-and-groove structure to large coral promontories and patches with low relief that extend into a large reef-front sand field. There is little disturbance due to incoming swell at this depth, and light levels remain high. At these depths, exposed fossil reef drops close to zero, while the living coral cover (%), species diversity, and morphology diversity reach a peak (Table 1). In this calm environment the rapidly growing, delicately branching *Porites compressa* dominates the coral community and *Montipora patula* is outcompeted by *Montipora capitata.*

Cored Lithofacies

Cores from both sites reveal five lithofacies (Fig. 3) that best describe the carbonate depositional environments associated with this study: encrusting coral–algal bindstone, mixed-skeletal rudstone, massive coral framestone, unconsolidated floatstone, and branching coral framestone–bafflestone.

Encrusting Coral–Algal Bindstone.—The main constituents of this lithofacies are fragments of *Montipora verrucosa, Montipora patula, Pocillopora meandrina,* and *Porites* sp., with occasional rudstones and rhodoliths bound together with coralline algae and heavy laminar micrite to form a solid framework (Fig. 4A). Fragments of brachiopods, gastropods (and other mollusks), and *Halimeda* sp. plates are also prevalent in this lithofacies. Major types of coralline algae are *Hydrolithon onkodes* and *Porolithon gardineri. Porolithon gardineri* in this lithofacies may act as a framebuilding as well as a binding component. Heavy laminar micrite encrusts and encapsulates pieces that may have initially been bound with thin coralline algae layers, suggesting late deposition of the micrite. Micrite is less prevalent near the benthic surface, indicating heavy flushing of the reef

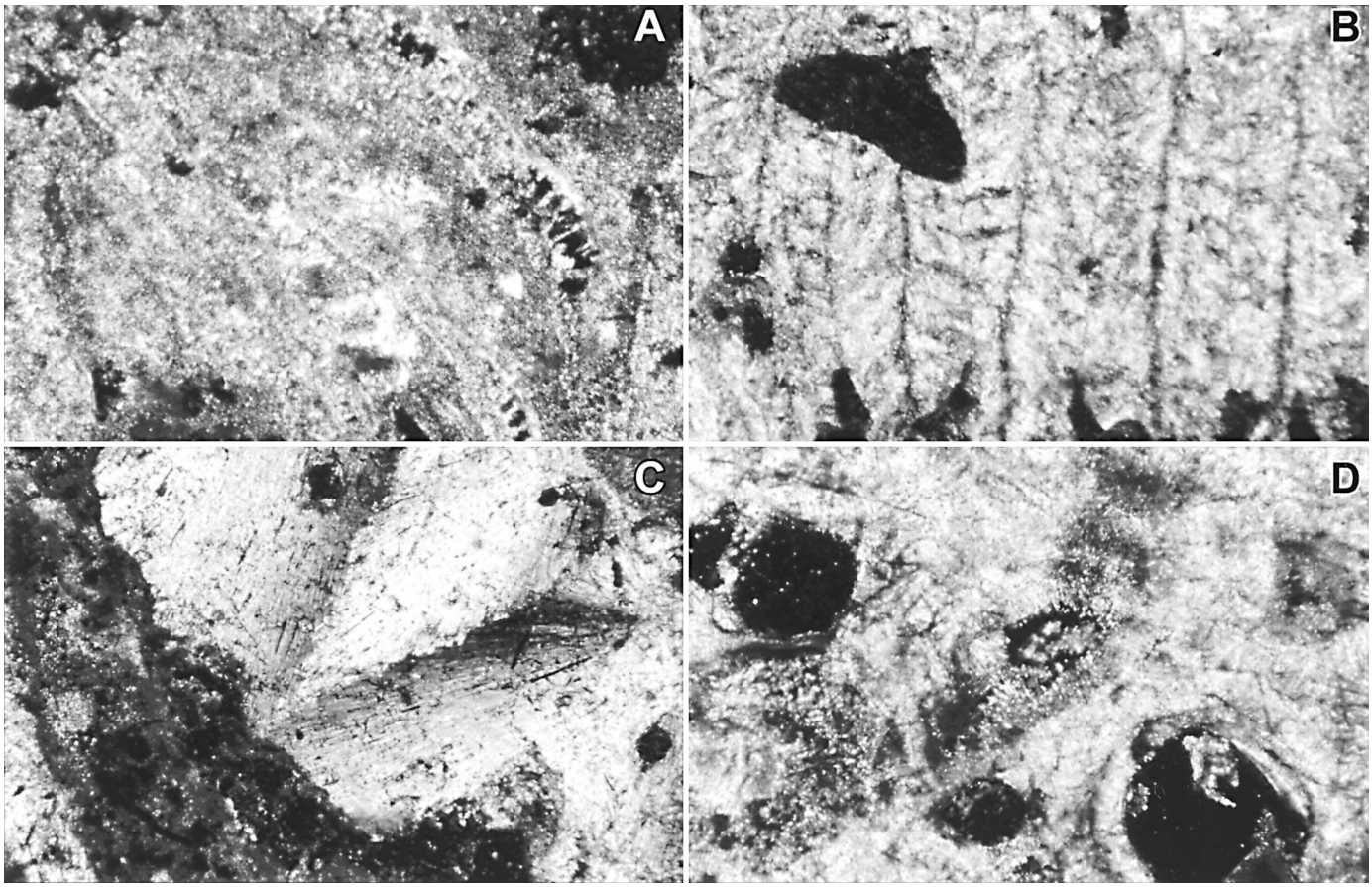

FIG. 4.—Lithofacies. **A)** Coral–algal bindstone from Hale O Lono (21 m depth) with encrusting coral and heavy laminar micritic cement displaying knobby texture. This lithofacies occurs at both HOL and Hikauhi. **B)** Massive coral framestone from Hikauhi (10.7 m depth). This lithofacies occurs only at Hikauhi. **C)** Mixed skeletal rudstone from Hale O Lono (8.5 m depth) showing brachiopod fragment and knobby micritic cement (lower left). This lithofacies occurs only at HOL. **D)** Branching coral framestone–bafflestone from Hale O Lono (17.7 m depth) showing bored, branching *Porites compressa* with aragonitic cement. This lithofacies occurs only at HOL.

structure in the upper sections and/or that micritization occurs at depth within the reef structure. This lithofacies occurs at both HOL and Hikauhi.

Mixed Skeletal Rudstone.—The components of this lithofacies are a mixture of unsorted, angular to rounded clasts of *Montipora capitata, Porites compressa, Pocillopora meandrina,* and rhodoliths of *Hydrolithon onkodes* from ~ 0.50 cm to ~ 5.00 cm in size. The lithofacies is unconsolidated, friable, and replete with *Halimeda* sp. plates, gastropods, brachiopods, and echinoderm spines. Coral pieces are generally worn and either lack encrustation or are heavily encrusted with *Hydrolithon onkodes* and micrite (Fig. 4C). Heavy encrustation by *Hydrolithon onkodes* suggests encrustation prior to deposition, while rubble is still exposed at the surface. Micrite coatings usually overlie algal encrustation. Coral pieces may be heavily bored by macro- and micro-boring organisms. This lithofacies occurs only at HOL.

Massive Coral Framestone.—Massive coral framestone is dominated by *Porites lobata* and *Porites* sp., most likely in growth position (Fig. 4B). In younger framestone there are few borings but the number increases with age. Borings may be filled with micrite stained with iron. This lithofacies occurs only at Hikauhi.

Unconsolidated Floatstone.—The dominant feature of this lithofacies is an unconsolidated sandy/muddy matrix that supports small (< 0.25 cm to ~2.00 cm), semi-rounded to rounded coral clasts. The matrix is dark brown to sandy gray in color with *Halimeda* sp. plates, brachiopods, and echinoderm spines. The predominant coral clasts, composed of *Porites compressa, Pocillopora meandrina, Pavona varians,* and *Montipora verrucosa,* are moderately to heavily bored, and encrusted with *Hydrolithon onkodes.* This lithofacies occurs only at Hikauhi.

Branching Coral Framestone–Bafflestone.—This lithofacies is composed predominately of *Porites compressa* in a delicate branching growth form and most likely in growth position. On the upper surfaces of the *Porites compressa* are encrustations of *Hydrolithon onkodes* ranging from < 0.25 cm to ~1.00 cm in thickness. The branching nature of *Porites compressa* acts as a baffle and traps echinoderm spines, brachiopods, *Porolithon gardineri* fragments, and *Halimeda* sp. flakes. Thick sequences of laminar micrite (~1–3 cm) have covered and infilled the branch cavities in this lithofacies. Very few borings traverse the thick layers of laminar micrite. The outermost surface of the micrite was deposited in a knobby texture similar to that described by Grossman (2001) and other authors, and is probably microbial in origin (Montaggioni and Camoin 1993). In these cores the upper surface of the exposed cavities in the top ~ 30 cm of cores are stained shades of brownish red. This lithofacies occurs only at HOL.

Subsurface Lithofacies Distribution and Dates

Hale O Lono: Early to Mid-Holocene Unit.—At HOL there are ten cores ranging in penetration depth (measured hole depth) below the seafloor from 0.76 to 2.30 m, with recovery ranging from 53% to 100% and averaging 80% (Fig. 5). Cores #1–4 and #8–10 are dominated by two lithofacies, mixed skeletal rudstone and encrusting coral–algal bindstone. HOL

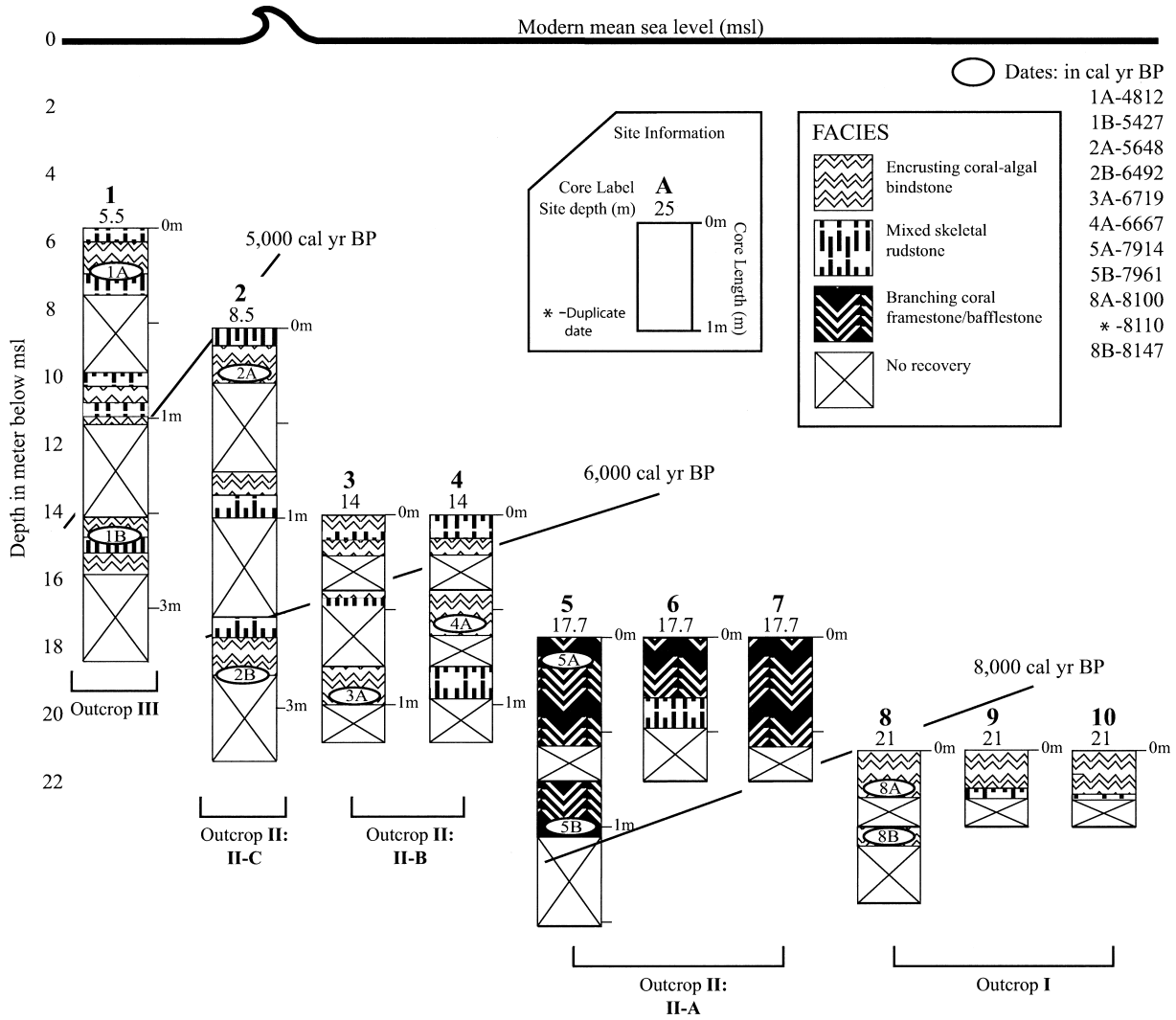

FIG. 5.—Drill-core lithologies and radiometric dates from Hale O Lono. Age of substrate increases with distance offshore. No modern ages are associated with this site, suggesting that little or no accretion has taken place since ~ 4,800 cal yr BP. Lithofacies associated with cores 5–7 are low-energy lithofacies, distinctly different from high-energy lithofacies that constitute the rest of the cores and implying a rapid rise in relative sea level prior to ~ 7,900 cal yr BP. Contours delineate regions of similar age.

cores #5, 6, and 7 are an exception to the lithology described above. These cores are dominated by branching coral framestone–bafflestone with a small amount of mixed skeletal rudstone.

Ten coral samples and one coralline algae sample were selected for XRD analysis and dating. All but one coral sample (H69-2-D2-B) contain > 90% aragonite (Table 2). The other component of these samples is magnesian calcite that ranges from 12.4 to 19.7 mole percent $MgCO_3$. The one coralline algae sample (H46-1-D2-B) consists solely of high-magnesian calcite with 35.5 mole percent $MgCO_3$. HOL dates range from 4,812 to 8,147 cal yr BP; sample ages decrease toward shore, and there are no inversions in the dates.

Micrite cements are dominant in these cores. The micrite occurs in three forms: peloidal micrite, microfossil micrite, and pelletized micrite. Peloidal micrite (cf. Sherman et al. 1999; Grossman 2001) is ubiquitous throughout the HOL cores (Fig. 4A), especially in cores #5–7, and constitutes the greater part of the micrite cements. Microfossil micrite is a micrite matrix embedded with crystalline carbonate clasts that are too small for source identification but which are assumed to be skeletal fragments (Fig. 4C). Pelletized micrite is solid micrite of uniform visual density or microfossil micrite overlain by small (< 0.10 um) pellets that appear to have a much greater visual density than the surrounding background.

Coralline algae also serves as a binding agent in these cores and often forms the first layer to encrust and bind pieces of coral rubble together. A unique feature of the coralline algae are its close association with pellets similar to those described for pelletized micrite. Given that these pellets are seen throughout the coralline algae structures and intermixed with different types of micrite, they may be biologically produced. Aragonite cement is rare in this reef unit and, where present, occurs as thin fibrous needles in interskeletal coral cavities.

Hikauhi: Late Holocene Unit.—At the Hikauhi site there are 14 cores with penetration depths (measured hole depth) from 0.76 to 5.33 m. Recovery ranged from 23% to 91% and averaged 56% (Fig. 6). All Hikauhi cores (A–N) are constructed of three lithofacies: massive coral framestone, coral–algal bindstone, and unconsolidated floatstone. Massive coral framestone and *Porites compressa* clasts throughout the unconsolidated floatstone are indicators of low-energy environments (Maragos 1977; Montaggioni and Camoin 1993; Maragos 1995; Grossman 2001). Coral–algal bindstone, usually an indicator of high-energy environments (Grossman 2001;

TABLE 2.—*Carbon 14 AMS ages and accretion rates.*

Core ID	Sample #	Type	Depth (m)	% Aragonite	$\delta^{13}C$	^{14}C Age (yrs)	^{14}C Error (yrs)	Calibrated ^{14}C age (yrs)	Cal age at 2(s)*** (yrs)	Accretion Rate (mm/yr)
1A	H18-D1-T	coral	5.72	100.00%	−0.88	4700	30	4812	4614–4935	2.26
1B	H18-D3-B	coral	7.11	91.28%	−0.59	5160	40	5427	5279–5553	—
2A	H28-D1-T	coral	8.77	100.00%	−1.89	5420	40	5648	5562–5840	1.86
2B	H28-D3-B	coral	10.34	95.71%	−1.65	6200	40	6492	6370–6654	—
3A	H46-1-D2-B	CA*	14.99	100%?	2.73	6390	30	6719	6591–6866	7.50
4A	Hale46-2A	coral	14.60	96.00%	−0.34	6350	55	6667	6646–6977	—
5A	Hale58-1A	coral	17.81	100.00%	0.1	7560	35	7914	7824–8116	23.40
5B	H58-1-D2-B	coral	18.91	92.24%	0.47	7640	40	7961	7844–8113	—
8A	Hale69-1A1	coral	21.27	97.00%	−0.56	7770	65	8110	8041–8323	4.83**
8A	Hale69-1A2	coral#	21.27	97.00%	0.06	7750	35	8100	7980–8325	—
8B	H69-1-D2-B	coral	21.47	89.01%	1.07	7800		8147	7992–8287	—
A1	R13-D1-B	coral	4.14	100.00%	0.15	>Mod		TYC	—	—
A2	R13-D4-B	coral	6.34	91.21%	1.42	795	30	303	229–463	6.04
A3	R13-D5-B	coral	7.53	100.00%	1.04	995	40	500	394–618	—
C1	R18-2-D1-T	coral	5.53	100.00%	−2.41	>Mod		TYC	—	—
C1	R18-2-D1-T	coral#	5.53	100.00%	−2	>Mod		TYC	—	—
C2	R18-2-D2-B	coral	6.84	86.64%	0.96	755	40	282	126–431	—
C2	R18-2-D2-B	coral#	6.84	86.64%	1.09	690	40	251	43–315	—
D1	R20-D2-M(1)	CA*	7.63	100%?	2.72	395	40	TYC	—	—
D2	R20-D2-M(2)	coral	7.70	93.44%	0.16	500	30	TYC	—	—
D3	R20-D2-B	coral	8.21	58.59%	2.44	580	50	60	0–237	2.67
D4	R20-D3-M	coral	8.79	97.05%	1.15	745	40	277	109–426	3.28
D5	R20-D4-M	coral	10.26	90.39%	0.85	1310	30	725	648–871	1.30
D6	R20-D4-B	coral	10.50	100.00%	−2.54	1470	30	910	760–1018	—
I1	R32-D2-T	coral	10.52	100.00%	−2.38	>Mod		TYC	—	—
I2	R2-D2-B	coral	11.18	100.00%	0.1	640	30	140	43–263	4.19
I3	R32-D4-B	coral	12.26	80.65%	0.56	850	30	398	280–473	—
K1	R42-D1-B	coral	13.19	100.00%	−2.49	>Mod		TYC	—	—
K2	R42-D2-B	coral	14.07	100.00%	−0.61	480	35	TYC	—	—
K3	R42-D4-B	coral	15.56	100.00%	0	790	35	300	222–458	—
N1	R65-D2-B	coral	21.02	100.00%	−1.79	595	40	83	0–238	2.10
N2	R65-D3-B	coral	21.89	100.00%	0.27	1000	30	502	419–609	—

* coralline algae, TYC–too young to calibrate, ? % calcite, # duplicate, ** Average of all replicates, *** Age range at 2 sigma.

reef-crest lithofacies of Kayanne et al. 2002), is restricted almost exclusively to cores from depths $<$ 10 m and is composed of multiple layers of encrusting coral. Hikauhi dates range from $<$ modern (too young to be dated by present techniques) to 910 cal yr BP. Ages at Hikauhi increase with depth but not with distance offshore. There are no inversions in the Hikauhi age data.

Twenty-one samples from this site were analyzed by XRD (Table 2). All but four samples have $>$ 90% aragonite. The remaining component is magnesian calcite with mole percent $MgCO_3$ from 7.88 to 18.90. The one sample of coralline algae (R20-D2-M1) consists solely of high-magnesian calcite with 17.49 mole percent $MgCO_3$. Dominant cements in these cores are peloidal micrite and microfossil micrite as described above with pelletized coralline algae acting as a binding agent. At Hikauhi, pelletized coralline algae are the dominant coral-clast binding agent, whereas peloidal micrite dominates first-generation pore infill and macroscale binding. Solution vugs and borings are rimmed with microfossil micrite, which is heavily stained red, possibly from a terrigenous iron source. The number and size of solution vugs increases with depth in the core. Although solution vugs are generally an indicator of freshwater dissolution, XRD analysis of the carbonate mineralogy, accurate within $\sim$ 1%, does not indicate the presence of low-magnesian calcite.

DISCUSSION

This discussion is presented in three parts. First we present a model for zonation of modern coral assemblages, followed by a comparison of the assemblage zonation and core lithofacies. Finally we present our interpretation of the paleo-history of the southwest corner of the Molokai reef as determined from lithofacies distribution.

Modern Assemblage Zonation

A correlation between wave energy, coral occurrence, and reef morphology has long been documented in the Hawaiian Islands (Dollar 1982; Rogers 1993; Grigg 1998), but Storlazzi et al. (2002) were the first to establish a quantitative physical model of the relationship in Hawaii. Storlazzi et al. (2002) modeled wave energy along Molokai's south shore using four dominant wave regimes: north swell, Kona storms, south swell, and trade-wind waves. HOL and Hikauhi, both located on the southwestern corner of the island, experience the same south, Kona, and trade-wind events. Major differences in wave energy between the two sites therefore result from exposure to refracted north swell that effects HOL but not Hikauhi.

To test the relative impact of north swell, Storlazzi et al. (2002) ran a nested wave model (WAM) (1.6 km by 1.6 km domain nested within a 1 degree by 1 degree global WAM) at the U.S. Naval Oceanographic Office to generate a gridded field of wave height, period, and direction for analysis. From these data, calculations were made of peak WINBSS under oscillatory flow (N/m^2), a measure of the wave force at the seafloor (Hardisty 1990; Storlazzi et al. 2002). These data were calculated for the entire south shore of Molokai at the 5 m, 10 m, 15 m, and 20 m isobaths (Fig. 7).

Measurements of bed shear stress were compared to rough visual estimates of coral type, percent coral cover, and reef width. Storlazzi et al. concluded that increasing WINBSS along Molokai's south shore correlates with changing coral community structure from finger-branching *Porites compressa*–dominated communities to more robust encrusting *Montipora* sp.–dominated communities to encrusting *Porites lobata* and stout branching *Pocillopora meandrina*–dominated communities. Additionally, increasing bed shear stress results in an overall reduction in percent living coral cover and diminishing reef width.

The model for zonation of modern coral assemblages seen at our study sites fits very nicely with data presented by Storlazzi et al. (2002). By combining physical observations obtained by Storlazzi et al. (2002) with seafloor surveys of this study, we define an assemblage zonation model for the southwest shore of Molokai consisting of three assemblages (Fig. 8); a low-energy assemblage, a mid-energy assemblage, and a high-energy as-

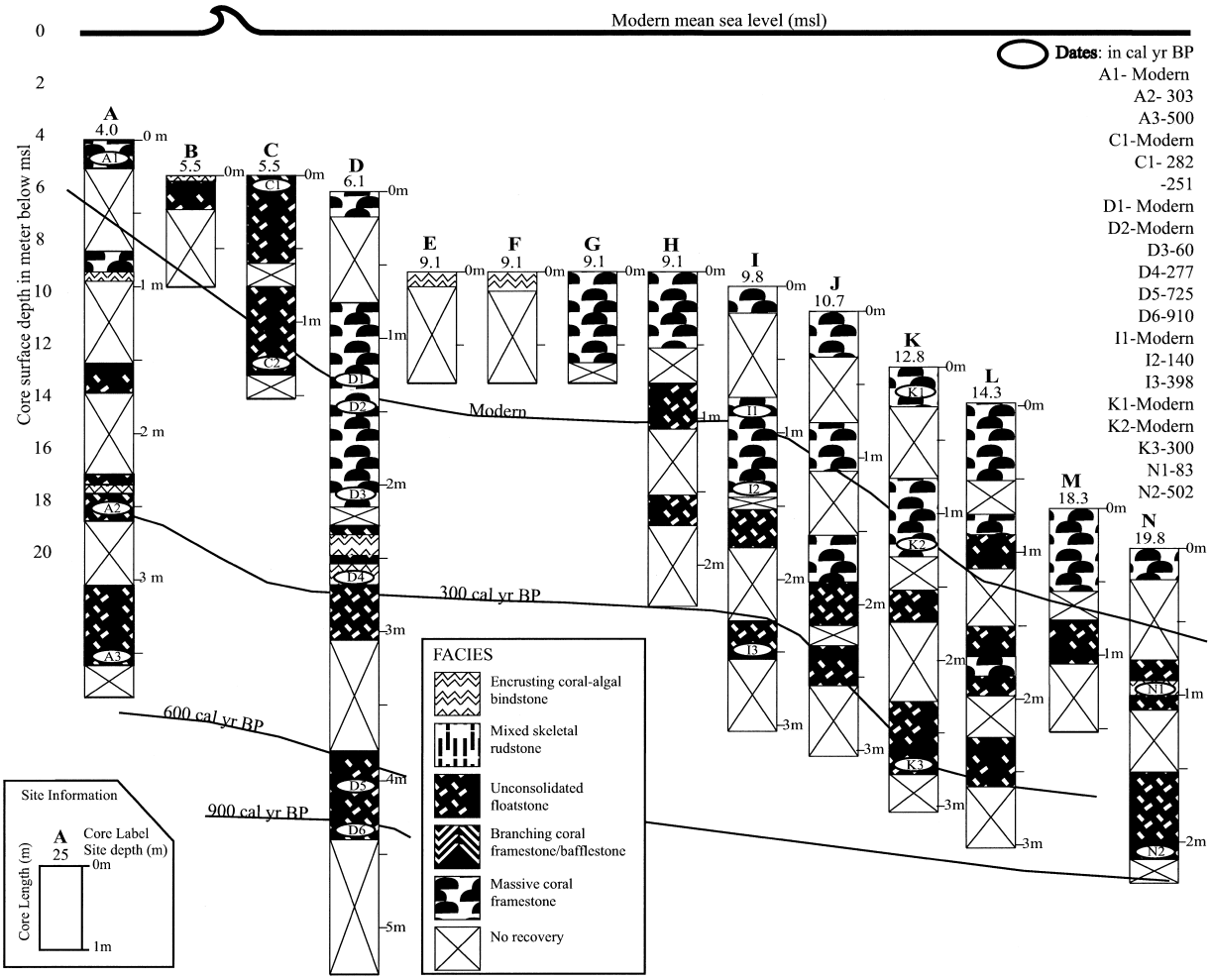

FIG. 6.—Drill-core lithologies and radiometric dates from Hikauhi. This site is a young (< 1,000 years) aggrading and prograding reef structure. The dominant lithofacies are unconsolidated floatstone and massive coral framestone. The volume of massive coral framestone is anomalous relative to the amount seen in the modern ecosystem because drill cores were specifically started on large *Porites lobata* heads in order to improve core recovery. Contours delineate regions of similar age and highlight the accreting nature of this reef structure.

semblage. The zonation model relates WINBSS (N/m^2) with percent living coral cover, percent coralline algae cover, dominant coral species, dominant coral morphologies, and water depth.

Each assemblage is divided into three depth zones, < 5 m, 5 m to 10 m, and > 10 m (to where the main reef structure ends). Although corals are only one part of the biota found along the seafloor, in general they constitute a majority of the community and thus are the dominant assemblage components described by this model. Those coral types that account for at least 10% of living coral cover are presented in the model. Finally, as with any assemblage zonation, there are considerable overlaps between zones, and considerable spatial variability due to local variation; hence, this model should be considered only a general classification.

Percent coralline algae cover, as presented in the model, is inversely related to water depth and directly related to WINBSS. Our observations show that in all three assemblages coralline algae has their highest representation in depths < 5 m, where bed stresses are highest. Additionally, coralline algae have greater representation in the high-energy assemblage than in the low-energy assemblage. This suggests that coralline algae are outcompeted by coral under conditions well suited to coral growth (conditions of lower wave energy) but that they flourish in conditions adverse to coral growth.

Low-energy assemblages, found to the east of Hikauhi in central portions of the island (data supplied by Storlazzi et al. 2002 and from personal communications with C. Storlazzi), with bed shear stresses ranging from < 0.2 to ~ 0.4 N/m^2, are dominated by *Porites compressa.* In Hawaii *Porites compressa* is generally regarded as a climax species in areas protected from heavy wave action. This coral, with rapid growth and thin columnar morphology, tends to outcompete other species (Maragos 1977). Coral cover in this assemblage is high and increases with depth, often approaching 100% at depths > 10 m. The other two coral species that appear in this assemblage are robust stout branching *Pocillopora meandrina,* in depths < 5 m, and massive *Porites lobata,* in depths to 5 m to 10 m.

As WINBSS increases to between ~ 0.3 to ~ 0.5 N/m^2, encrusting *Montipora* species begin to compete with *Porites compressa* for space in the mid-energy assemblage, represented by Hikauhi. *Montipora* sp. are described by Maragos (1977) to be generalists, inhabiting depths from 0 to 50 m, occurring in a range of energetic conditions and assuming a multitude of growth forms. Encrusting forms are most commonly seen in this assemblage as the coral grows in and around the bases of the branching *Porites compressa.* We speculate that by growing around the base of the *Porites compressa,* the *Montipora* sp. may actually be providing some skeletal strength to the *Porites compressa,* allowing it to grow in environments with greater bed shear stress than is ideal for this species. Dominant coral types

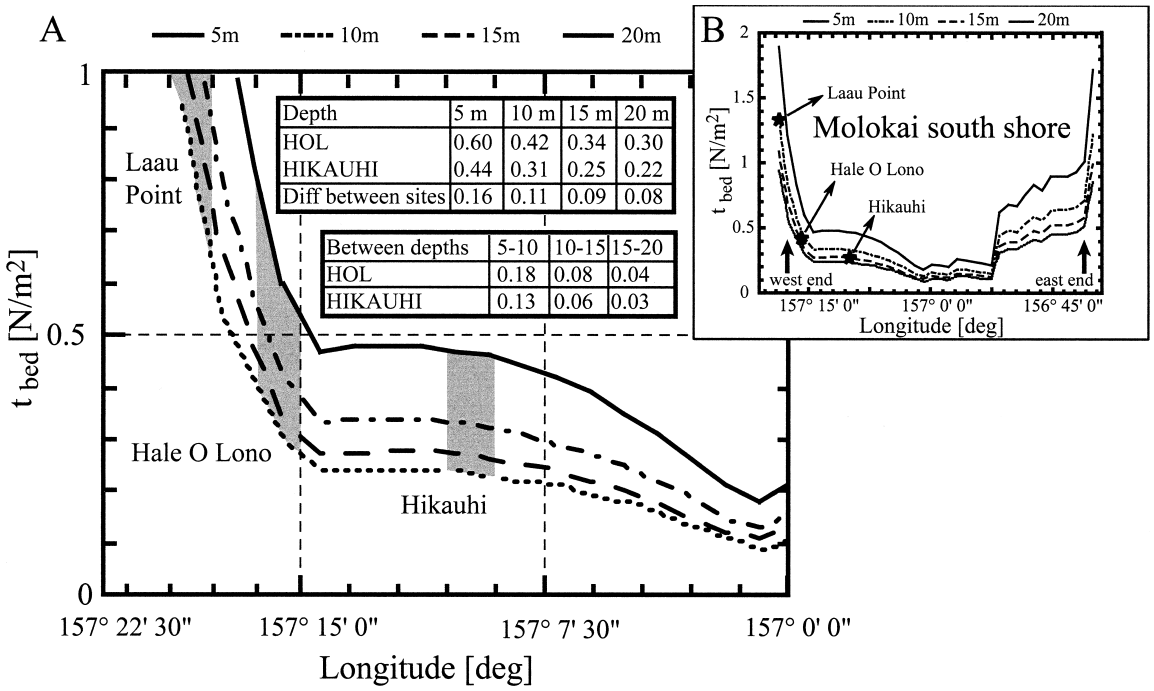

Depth	5 m	10 m	15 m	20 m
HOL	0.60	0.42	0.34	0.30
HIKAUHI	0.44	0.31	0.25	0.22
Diff between sites	0.16	0.11	0.09	0.08

Between depths	5-10	10-15	15-20
HOL	0.18	0.08	0.04
HIKAUHI	0.13	0.06	0.03

FIG. 7.—**A)** Plot of modeled bed shear stress (WINBSS) due to north swell as a function of water depth along the southwest shore of Molokai. Gray shading denotes Laau Point, Hale O Lono, and Hikauhi. Bed shear stress is presented in the associated table for 5 m, 10 m, 15 m, and 20 m isobaths. The difference in bed shear stress between HOL and Hikauhi at each isobath and between isobaths are also presented. **B)** Inset shows the WINBSS from north swell for the entire south shore of Molokai (after Storlazzi et al. 2002).

change in water depths < 5 m where *Pocillopora meandrina* becomes a significant assemblage component, though in depths > 10 m *Porites lobata* in massive form is the interloper. As with the low-energy assemblage, percent living coral cover in the mid-energy assemblage increases with depth.

At bed stresses from ~ 0.4 N/m^2 to ~ 0.6 N/m^2 there is a shift to the high-energy assemblage such as the HOL site. Fragile branching *Porites compressa* disappears completely from the dominant corals, being replaced by *Montipora* sp., *Pocillopora meandrina,* and encrusting *Porites lobata.* At depths > 10 m, *Porites lobata* in encrusting and massive forms takes over as the dominant coral as *Montipora* sp. and *Pocillopora meandrina* diminish. This assemblage is characterized by low living coral cover and, unlike mid-energy and low-energy assemblages, has an optimum for coral growth between 5 m and 10 m water depth. There is surprising continuity across a range of depths in this assemblage. Even though WINBSS at depths > 5 m is similar to that seen in the mid-energy and low-energy assemblages, the coral grouping remains very different. Boundaries between the mid-energy and low-energy assemblages are less distinct than those between mid-energy and high-energy assemblages.

Although the model provides a good description of general coral zonation, WINBSS is not the sole factor controlling type and location of coral growth along the southwest shore of Molokai. For example, although increasing WINBSS explains decreasing coral cover in shallow water for both mid-energy and low-energy assemblages, the high-energy assemblage does not fit the expected profile, inasmuch as the lowest percentage coral cover is at the greatest depths (Table 1). Additionally, although habitat in the high-energy assemblage has regions suitable to growth of *Porites compressa* (Fig. 8), this coral is not a major component of the seafloor. Some possible explanations for these differences may be related to interruption of coral recruitment and physical degradation of living coral by sources other than WINBSS.

The substrate available for colonization at HOL is an antecedent paleoreef platform that forms shore-parallel bands interspersed with large sand fields. Height differences between the paleoreef platforms and the sand fields are usually < 1 m, and *Halimeda* sp. which might bind the sediment (bound *Halimeda* sp. mats are common in Hawaii; Harney 2000), are scarce. Refracted north swell regularly sweeps these sand fields and carbonate platforms, suspending coarse carbonate sediment and coral rubble. Although coarse suspended sediment remains low in the water column, sites of coral recruitment do not have sufficient relief to place them above the sediment cloud. Additionally, as sediment sweeps back and forth it physically abrades the seafloor. The abrasive action likely disrupts recruitment activities and significantly slows growth rates by chafing any established living coral. We speculate that coral rubble accelerated by wave energy, in addition to the physical abrasion of the reef surface, acts ballistically, smashing coral that might otherwise survive sand abrasion. Hence we speculate that physical disturbance of recruitment processes, and physical degradation of the established living communities, in addition to elevated WINBSS at shallow depth, combine to limit living coral cover at HOL (Table 1).

Lithofacies

Reef cores from HOL and Hikauhi contain components very similar to those found in the modern reef community. When compared with the modern assemblage zonation, lithofacies components allow identification of probable past depositional environments.

Common to both coral–algal bindstone and mixed skeletal rudstone are heavy encrustations of coralline algae, small coral clasts that have been significantly rounded, and no indication of corals in growth position. This suggests that a modern analog for the depositional environment of these lithofacies is the high-energy coral communities seen at HOL today.

Coral framestone lithofacies are composed predominantly of one coral species, massive *Porites lobata.* Massive *Porites lobata* in the modern environment grows in all three modern ecosystem communities, but it seems to prefer calmer water at depths > 5 m (> 10 m for high-energy com-

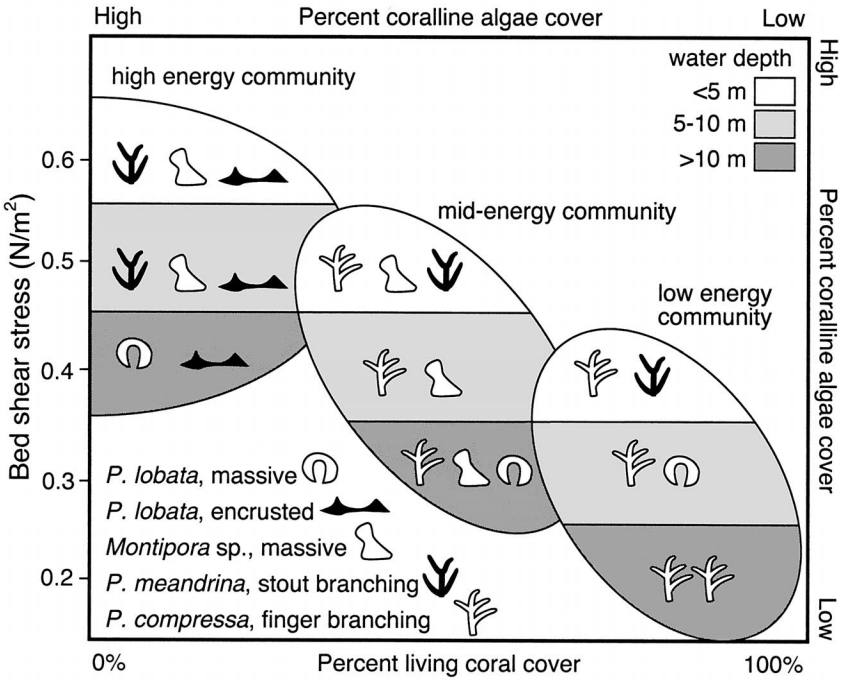

FIG. 8.—Model of modern coral assemblage zonation. This model relates bed shear stress (WINBSS) with percent living coral cover, dominant coral species, and coral morphologies. The low-energy community is dominated by *Porites compressa,* especially at depths > 5 m, and is found along the central portions of the south shore of Molokai. To the west, bed shear stress increases and the ecosystem shifts to a mid-energy community, as at Hikauhi, dominated by *Porites compressa* and *Montipora* sp. At the westernmost site, Hale O Lono, near the western end of the island where bed shear stresses increase sharply, the high-energy community is dominated by *Porites lobata, Pocillopora meandrina,* and *Montipora* sp.

munities). In cored section however, it is not always easy to differentiate encrusting from massive morphologies of *Porites lobata* by skeletal comparison. The depositional environments for encrusting *Porites lobata* tend to be high-energy environments near the reef crest or toward the end of the island, distinctly contrasting with massive *Porites lobata.* Fortunately in the modern environment encrusting *Porites lobata* has low vertical relief, whereas massive *Porites lobata* has much higher relief. Thus, for this study, any section of *Porites lobata* 15 cm in height or less was identified as encrusting *Porites lobata* and is interpreted as coral–algal bindstone within a high-energy depositional environment. An example of this occurs in the top section of core #8 (HOL), composed of three separate colonies of encrusting *Porites lobata.*

Unconsolidated floatstone, a mixture of rubble suspended in a sediment matrix, is likely deposited in a moderate-energy environment. This lithofacies is ubiquitous throughout the reef at Hikauhi, in places reaching the surface, and consistently dates younger than 1,000 cal yr BP. Also, coral types identified in this lithofacies are similar to the coral types identified in our benthic surveys from Hikauhi. Thus we infer that moderate-energy communities, as at Hikuahi, are the predominant depositional environment for this lithofacies.

Finally, *Porites compressa* is the dominant structural component of the coral framestone–bafflestone lithofacies. Hence we would expect the depositional environment for this lithofacies to be conducive to growth of *Porites compressa* and sheltered from wave impacts. Where this lithofacies has been identified in our cores, *Porites compressa* shows no close association with *Montipora* sp., which would be expected if this lithofacies were deposited in a mid-energy community. Additionally, because fragile thin columnar coral appears to have been deposited in growth position, the depositional environment for this lithofacies is likely to be deep or calm substrates like those seen today in low-energy communities of central southern Molokai.

Holocene Reef Accretion

Early and Mid-Holocene (9,000 to 4,000 cal yr BP).—The early to mid-Holocene reef at HOL was characterized by a pattern of backward-stepping reefal limestone outcrops that decrease in age toward shore. In addition to this transgressive sequence, accretion on any given outcrop appears to have ceased with initiation of a new accretion center in a shoreward direction.

Some time before 8,000 cal yr BP at HOL, a reef community, actively accreting (5 mm/yr), was established at a present depth of—21 m (Fig. 9). This community, now exposed as outcrop I (cores #8–10), is composed of encrusting coral–algal bindstones intermixed with occasional *Porites* sp. and mixed skeletal rudstones. This lithofacies indicates a high-energy depositional setting, similar to the modern high-energy community seen today at HOL. These same groupings have been described by Maragos (1995) and Grossman (2001) as high-energy lithofacies (see also Camoin and Montaggioni 1994 and Cabioch et al. 1999 for Indo-Pacific similarities), usually deposited near the reef crest. Carbonate accretion at this outcrop terminated at ~ 8,100 cal yr BP.

Outcrop II, ranging in depth from ~ 8 m to ~ 18 m, is 125 m landward of outcrop I. Sometime prior to ~ 7,900 cal yr BP accretion started taking place on the lower flank of II at site II-A (cores #5–7). Site II-A accreted upward at a rate of 23 mm/yr until accretion ended at ~ 7,900 cal yr BP. This rapid vertical accretion is recorded in the coral framestone–bafflestone lithofacies present throughout cores #5–7. Branching coral framestone–bafflestone is indicative of low-energy environments as noted in this study as well as by Dollar (1982), Grigg (1983), and Grossman (2001) (as well as in other Indo-Pacific studies, i.e., Cabioch et al. 1999). Grossman (2001) found this same lithofacies on the seaward edge of Kailua Bay, Oahu, in a portion of the reef characterized by early Holocene rapid vertical accretion. The presence of branching coral framestone–bafflestone suggests that water levels changed rapidly enough to produce a deep-water condition where the energy was low enough to be conducive to branching growth of *Porites compressa.*

Sometime between ~ 7,900 cal yr BP and ~ 6,700 cal yr BP the middle section of outcrop II, site II-B (cores #3–4), was accreting vertically at rates of 9 mm/yr. The lithofacies of this section, consisting of coral–algal bindstone and mixed skeletal rudstone, are very similar to lithofacies seen in outcrop I. This implies a return to moderate-energy to high-energy conditions at this site. By ~ 6,600 cal yr BP all upward accretion at this site ended.

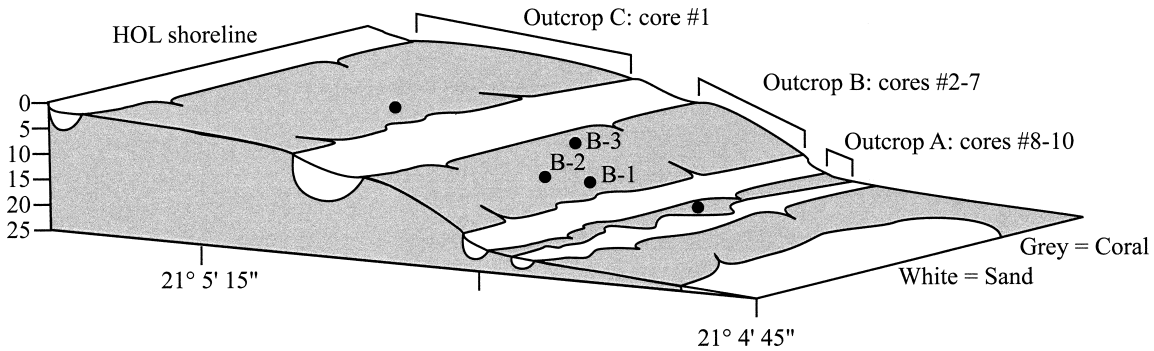

FIG. 9.—Overview of reef outcrops present at Hale O Lono. Interspersed between rocky outcrops are sand fields that are regularly swept by large waves and strong currents. Because vertical relief is quite low, suspended carbonate sediment physically abrades the reef surface. Cores taken at II-A (#5–7) show anomalous low-energy branching coral framestone–bafflestone lithofacies, whereas the remaining cores are composed of lithofacies indicating high-energy depositional environments.

After accretion ended at site II-B, the accretion center shifted landward to the upper flank of outcrop II, at site II-C (core #2). Once accretion ended at site II-C (~ 5,600 cal yr BP), there was another landward shift of the accretion center to outcrop III (core #1). Site II-C and outcrop III are similar in composition to outcrop I and site II-B but have accretion rates of only ~ 2 mm/yr, the lowest for any of the cores, and implying either a slowing in the rate of RSLR or a strengthening of wave energy. Outcrop III appears to be the last major accretion center in this area during the mid-Holocene. Since ~ 4,800 cal yr BP, little or no accretion has taken place at HOL.

Factors Controlling Early to Mid-Holocene Accretion at HOL.—We infer that relative sea-level rise at HOL is only partially responsible for controlling accretion over early to mid-Holocene time. The landward transgressive shift of reef outcrops can be explained by rising relative sea levels. This, however, does not explain the end of accretion on deeper, more seaward outcrops, occurring coincidently (or nearly so) with establishment of a new accretion center landward.

The high-energy lithofacies of outcrop I (~ 8,100 cal yr BP) suggest deposition near sea level. This would likely place site II-A (landward of I) in a supratidal range and the other outcrops above the waterline for the same period. Between ~ 8,100 cal yr BP and ~ 7,900 cal yr BP outcrop I experienced no accretion, but during that same period site II-A was an environment conducive to growth of nearly monospecific stands of *P. compressa.* Our assemblage zonation model indicates that monospecific stands of *Porites compressa* grow in deep water in moderate- to low-energy environments. *Porites compressa* does grow in other environments, and it is possible to find stands of monospecific *Porites compressa* at shallower depths, though usually of limited extent and restricted to moderate- to low-energy environments. The presence of branching coral framestone–bafflestone in three separate cores suggests that this was not an isolated patch of *Porites compressa,* but rather an extensive feature. Hence we infer that between ~ 8,100 cal yr BP and ~ 7,900 cal yr BP sea level rose rapidly to produce the deep calm substrates necessary for the growth of *Porites compressa.* This is not an anomalous finding, inasmuch as evidence for rapid rise in sea level close to this time has been previously described in the literature, though there is significant variation regarding timing and magnitude of the event (Blanchon and Shaw 1995; Kayanne et al. 2002; Blanchon et al. 2002).

Sometime between ~ 7,900 cal yr BP and 6,600 cal yr BP, perhaps as the rate of RSLR decreased, the accretion center at site II-A was abandoned in favor of the more landward, II-B accretion center. The shift from the II-B to the II-C accretion center (between ~ 6,600 cal yr BP and ~ 5,600 cal yr BP), and from II-C to III accretion center (between ~ 5,600 cal yr BP and ~ 4,800 cal yr BP) occurred under slowly rising sea level as seen by the presence of high-energy lithofacies and very slow accretion rates (~ 2 mm/yr for III and II-C and ~ 9 mm/yr for II-B).

Relative sea-level change explains the transgressive nature of the reef system at HOL, but it does not explain the unique pattern of increasing benthic surface age with distance offshore. The vertical relief between sites is small enough (~ 2 m to ~ 4 m) that we would expect continued accretion across the entire structure under slowly rising sea levels, but we find no evidence for this. One possible explanation is a progressive decrease in wave sheltering from north swell by Laau Point. The bathymetry at Laau Point, ~ 5 km west of HOL, is a broad, shallow shelf that grades to the southwest onto a large carbonate bank at—50 m. With sea level at ~ 20 m below present at ~ 8,100 cal yr BP, the exposed surface of Laau Point would have extended a full kilometer to the west of its present position. Although it has not been modeled, we infer that this may have been sufficient to shelter HOL from the main energy of north swell. Outcrop I was established under these conditions. With sea-level rise, the extent of sheltering from north swell would have been reduced with progressive drowning of Laau Point, and accretion centers would have been forced to migrate landward to find habitat suitable for sustained growth. Continued sea-level rise would have set up a cycle of reef accretion on progressively landward sites with accretion terminating at former accretion centers.

The Laau Point model does not address the absence of continued reef accretion during middle to late Holocene time. We must invoke a factor beyond sea-level rise and wave sheltering to account for this difference. Two possibilities are (1) increasingly steep topography and (2) changes in the energy associated with north swell. While the bathymetry below Laau Point is gradual, 20 m over 1 km, the present topography above the point is much more dramatic, 20 m in ~ 0.27 km. With continued inundation during the Kapapa Stand (the late middle Holocene sea-level highstand in Hawaii; Fletcher and Jones 1996; Grossman and Fletcher 1998; Grossman et al. 1998), the steep topography directly inland of HOL would have opened up relatively little new substrate to colonization, and deepening waters at the point would have allowed more north swell energy to be refracted around Laau Point. The other possibility is strengthening of the north swell over the course of the middle to late Holocene time, perhaps due to strengthening of El Nino Southern Oscillation (ENSO) (Sandweiss et al. 1996; Rodbell et al. 1999; Sandweiss et al. 1999; Moy et al. 2002; Rooney et al. 2003).

Mid to Late Holocene: 5,000 to Present.—The major unconformity represented by the ca. ~ 4,800 cal yr BP age seafloor spans middle to late Holocene time at HOL. Complete absence of accretion during this period attests that the environment was not conducive to reef growth. The only late Holocene age samples were recovered from Hikauhi. Here the accretion patterns are not nearly as complex as HOL.

The main accretionary feature at Hikauhi is the growth of the reef structure through combined aggradation and progradation as evidenced by the decrease in age of isochrons in both upward and seaward directions. At the reef crest vertical accretion has reached the intertidal zone. This has resulted

in a seaward shift of the Hikauhi accretion center resulting in lateral and vertical extension dominating reef growth over the last 1,000 yr. In the absence of north swell, the main control on reef growth at this site is limited vertical accommodation space and lateral substrate suitable for colonization (a large sand field fronts much of the reef). Where early to mid-Holocene units are situated at this site is not known, but we speculate that they would be below what is presently the backreef area.

CONCLUSIONS

Reef history at Hale O Lono and Hikauhi on Molokai is revealed by combining cored lithofacies with modern community surveys to develop an analytical model of the relationship of carbonate accretion patterns to past environmental conditions. At both Hale O Lono and Hikauhi the modern community is zoned by depth: $<$ 5 m, 5–10 m, and $>$ 10 m. At Hale O Lono, coral cover, species diversity, and growth morphology diversity all peak between 5 and 10 m and diminish sharply above and below this zone. At Hikauhi, coral cover, species diversity, and growth morphology diversity all peak at depths $>$ 10 m and decrease toward shore.

The main control on modern ecosystem zonation in southwest Molokai is the exposure to wave-induced near-bed shear stress. As bed shear stresses increase, the coral community changes from a low-energy community dominated by *Porites compressa,* to a mid-energy community dominated by mixed *Porites compressa* and *Montipora* sp., to a high-energy community dominated by *Porites lobata, Montipora* sp., and *Pocillopora meandrina.* Additionally, coralline algae cover increases with increasing bed shear stress and decreasing living coral cover. Other factors controlling coral assemblage zonation are success of recruitment activities and physical degradation of the living community by abrasion.

Reef lithofacies, determined by comparison of modern assemblage zonation to lithologic components of reef cores from both Hale O Lono and Hikauhi, are dominated by five classes corresponding to differing environmental conditions. In order of decreasing depositional energy they are: encrusting coral–algal bindstone and mixed-skeletal rudstone (high-energy environment), massive coral framestone (moderate energy), unconsolidated floatstone (moderate-energy environment), and branching coral framestone–bafflestone (low-energy environment).

Reef accretion at Hale O Lono during early Holocene time occurred in discrete events, with accretion centers stepping landward under relative sea-level rise. Rising sea levels, responsible for opening new habitat for colonization, exhibited variable rates throughout early to middle Holocene time. We infer from lithofacies that between $\sim$ 8,100 cal yr BP and $\sim$ 7,900 cal yr BP sea level rose sharply to produce deep calm substrates necessary for the growth of *Porites compressa* in monospecific stands. Sea-level rise also contributed to the termination of former accretion centers by reducing wave sheltering associated with Laau Point. At $\sim$ 4,800 cal yr BP, increasing vertical topography and possibly increased wave energy associated with north swell ended significant reef accretion at Hale O Lono. The record at Hale O Lono strongly supports the hypothesis of Rooney et al. (2003) that enhancement of the El Niño Southern Oscillation beginning approximately 5000 years ago led to increased energy of north swell and signaled the end to net accretion along exposed coastlines in Hawaii. The exposure of Hale O Lono to north swell and the age of sea floor there (ca. 4,800 cal yr BP), coupled with the lack of north swell incidence at Hikauhi and the continuous accretion that has occurred there over the last millennium strongly supports the ENSO reef hypothesis as outlined by Rooney et al. (2003).

The reef at Hikauhi has both aggraded vertically and prograded seaward over the past 1,000 yr. The impact of bed shear stress at Hikauhi is significantly lower compared to Hale O Lono. Accommodation space below wave base rather than wave energy appears to be the major factor controlling reef growth at Hikauhi in shallow depths. At greater depths, reef growth is limited by substrate suitable for colonization due to sediment accumulation at the base of the reef at depths $>$ 17 m.

Age discrepancies between HOL and Hikauhi make direct comparison of accretion histories impossible. Analysis of these sites together, however, yields a picture of shrinking habitat suitable for reef accretion during the Holocene.

ACKNOWLEDGMENTS

This work was supported by the U.S. Geological Survey (Award No. 98WARG1030) and the N.O.A.A. Hawaii Coral Reef Initiative Research Program (Award No. NA160A1449). The first author was supported by a graduate fellowship awarded by the Khaled Bin Sultan Living Oceans Foundation. Thanks also to the crew of the M.Y. *Golden Shadow,* and the R/V *Alyce C.* Special thanks to Jodi Harney (USGS), Mathew Barbee, and Jane Schoonmaker (UH), and captains Alan Weaver and Joe Reich.

REFERENCES

Bischoff, J.L., Bishop, F.C., and Mackenzie, F.T., 1983, Biogenically produced magnesian calcite: inhomogeneities in chemical and physical properties; comparison with synthetic phases: American Mineralogist, v. 68, p. 1183–1188.

Blanchon, P., and Shaw, J., 1995, Reef drowning during the last deglaciation: Evidence for catastrophic sea-level rise and ice-sheet collapse: Geology, v.23, p. 4–8.

Blanchon, P., Jones, B., and Ford, D.C., 2002, Discovery of a submerged relic reef and shoreline off Grand Cayman: further support for an early Holocene jump in sea level: Sedimentary Geology, v. 147, p. 253–270.

Cabioch, G., Montaggioni, L.F., Faure, G., and Ribaud-Laurenti, A., 1999, Reef coralgal assemblages as recorders of paleobathymetry and sea level changes in the Indo-Pacific province: Quaternary Science Reviews, v. 18, p. 1681–1695.

Camoin, G.F., and Montaggioni, L.F., 1994, High energy coralgal–stromatolite frameworks from Holocene reefs (Tahiti, French Polynesia): Sedimentology, v. 41, p. 655–676.

Clague, D.A., 1998, Moloka'i and Lanai, *in* Juvik, S.P., and Juvik, J.O., eds., Atlas of Hawaii, Third Edition: Honolulu, University of Hawaii Press, p. 11–13.

Cortes, J., Macintyre, I.G., and Glynn, P.W., 1994, Holocene growth history of an eastern Pacific fringing reef, Punta Islotes, Costa Rica: Coral Reefs, v. 13, p. 65–73

Dollar, S.J., 1982, Wave stress and coral community structure in Hawaii: Coral Reefs, v. 1, p. 71–81.

Dollar, S.J., and Tribble, G.W., 1993, Recurrent storm disturbance and recovery: A long-term study of coral communities in Hawaii: Coral Reefs, v. 12, p. 223–233.

Dunham, R.J., 1962, Classification of carbonate rocks according to depositional texture, *in,* Ham, W.E., ed., Classification of Carbonate Rocks: American Association of Petroleum Geologists, Memoir 1, p. 175–192.

Easton, W.H., and Olson, E.A., 1976, Radiocarbon profile of Hanauma Reef, Oahu, Hawaii: Geological Society of America, Bulletin, v. 78, p. 711–719.

Embry, A.F., and Klovan, J.E., 1971, A Late Devonian reef tract on north-eastern Banks Island, N.W.T.: Bulletin of Canadian Petroleum Geology, v. 19, p. 730–781.

Fairbanks, R.G., 1989, A 17,000-year glacio-eustatic sea level record: influence of glacial melting rates on the Younger Dryas event and deep-ocean circulation: Nature, v. 342, p. 637–642.

Fletcher, C.H., and Jones, A.T., 1996, Sea-level highstand recorded in Holocene shoreline deposits on Oahu, Hawaii: Journal of Sedimentary Research, v. 66, p. 632–641.

Fletcher, C.H., Grossman, E.G., Sherman, C.E., Harney, J.N., Rubin, K., Murry-Wallace, C., and Edwards, L., 2001, Complex origin and structure of the Oahu carbonate shelf: Hawaiian Islands: Abstracts with Programs, Geological Society of America, Annual Meeting, Boston, v. 33, p. A-408.

Grigg, R.W., 1983, Community structure, succession and development of coral reefs in Hawaii: Marine Ecology Progress Series, v. 11, p. 1–14.

Grigg, R.W., 1998, Holocene coral reef accretion in Hawaii: a function of wave exposure and sea level history: Coral Reefs, v. 17, p. 263–272.

Grigg, R.W., and Jones, A.T., 1997, Uplift caused by lithospheric flexure in the Hawaiian Archipelago as revealed by elevated coral deposits: Marine Geology, v. 141, p. 11–25.

Grossman, E.G., 2001, Holocene sea level history and reef development in Hawaii and the central Pacific Ocean [Ph.D. Thesis]: University of Hawaii, Geology and Geophysics, 256 p.

Grossman, E.G., and Fletcher, C.H., 1998, Sea level higher than present 3500 years ago on the northern main Hawaiian Islands: Geology, v. 26, p. 363–366.

Grossman, E.G., Fletcher, C.H., and Richmond, B.M., 1998, The Holocene sea-level highstand in the equatorial Pacific: analysis of the insular paleosea-level database: Coral Reefs, v. 17, p. 309–327.

Hardisty, J., 1990, Beaches: Form and Process: London, Unwin Hyman Ltd, 324 p.

Harney, J., 2000, Carbonate Sedimentology of a windward shoreface: Kailua Bay, Oahu, Hawaiian Islands [Ph.D. Thesis]: University of Hawaii, Geology and Geophysics, 232 p.

Hearty, P.J., Kaufman, D.S., Olson, S.L., and James, H.R., 2000, Stratigraphy and whole-rock amino acid geochronology of key Holocene and last interglacial carbonate deposits in the Hawaiian Islands: Pacific Science, v. 54, p. 423–442.

Jones, A.T., 1993, Review of the chronology of marine terraces in the Hawaiian Archipelago: Quaternary Science Reviews, v. 12, p. 811–823.

KAYANNE, H., YAMANO, H., AND RANDALL, R.H., 2002, Holocene sea-level changes and barrier reef formation on an oceanic island, Palau Islands, western Pacific: Sedimentary Geology, v. 150, p. 47–60.

MACINTYRE, I.G., 1975, A diver-operated hydraulic drill for coring submerged substrates: Atoll Research Bulletin, v. 185, p. 21–26.

MARAGOS, J.E., 1977, Order Scleractinia: stony corals, *in* Devaney, D.M., and Eldredge, L.G., eds., Reef and Shore Fauna of Hawaii: Honolulu, Bishop Museum Press, p. 158–241

MARAGOS, J.E., 1995, Revised checklist of extant shallow-water stony coral species from Hawaii (Cnidaria: Anthozoa: Scleractinia): Bishop Museum, Occasional Papers, v. 2, p. 54–55.

MARAGOS, J.E., 1998, Marine Ecosystems, *in* Juvik, S.P., and Juvik, J.O., eds., Atlas of Hawaii, Third Edition: Honolulu, University of Hawaii Press, p. 111–120.

MONTAGGIONI, L.F., AND CAMOIN, G.F., 1993, Stromatolites associated with coralgal communities in Holocene high-energy reefs: Geology, v. 21, p. 149–152.

MONTAGGIONI, L.F., AND FAURE, G., 1997, Response of reef coral communities to sea-level rise: a Holocene model from Mauritius (Western Indian Ocean): Sedimentology, v. 44, p. 1053–1070.

MONTEBON, A.R.F., 1992, Use of the line intercept technique to determine trends in benthic cover: 7th International Coral Reef Symposium Proceedings, Guam, v. 1, p. 151–155.

MOORE, J.G., BRYAN, W.B., AND LUDWIG, K.R., 1994, Chaotic deposition by a giant wave, Molokai, Hawaii: Geological Society of America, Bulletin, v. 106, p. 962–967.

MOY, C.M., SELTZER, G.O., RODBELL, D.T., AND ANDERSON, D.M., 2002, Variability of El Nino/Southern Oscillation activity at millennial timescales during the Holocene epoch: Nature, v. 420, p. 162–165.

MUHS, D.R., AND SZABO, B.J., 1994. New uranium-series ages of the Waimanalo limestone, Oahu, Hawaii: Implications for sea level during the last interglacial period: Marine Geology, v. 118, p. 315–326.

OGSTON, A.S., STORLAZZI, C.D., FIELD, M.E., AND PRESTO, M.K., in press, Currents and suspended sediment transport on a shallow reef flat: South-central Molokai, Hawaii: Coral Reefs.

RODBELL, D.T., SELTZER, G.O., ANDERSON, D.M., ABBOTT, M.B., ENFIELD, D.B., AND NEWMAN, J.H., 1999, An ~ 15,000-year record of El Nino–driven alluviation in southwestern Ecuador: Science, v. 283, p. 516–520.

ROGERS, C.S., 1993, Hurricanes and coral reefs: The intermediate disturbance hypothesis revisited: Coral Reefs, v. 12, p. 127–138.

ROONEY, J.J.R., FLETCHER, C.H., GROSSMAN, E., ENGELS, M., AND FIELD, M., 2003, El Nino control of Holocene reef accretion in Hawaii: Pacific Science, v. 58, p. 305–324.

RUBIN, K.H., FLETCHER, C.H., AND SHERMAN, C., 2000, Fossiliferous Lana'i deposits formed by multiple events rather than a single giant tsunami: Nature, v. 408, p. 675–681.

SABINE, C.L., 1992, Geochemistry of particulate and dissolved inorganic carbon in the central North Pacific [Ph.D. thesis]: University of Hawaii, 250 p.

SANDWEISS, D.H., MAASCH, K.A., AND ANDERSON, D.G., 1999, Transitions in the Mid-Holocene: Science, v. 283, p. 499–500

SANDWEISS, D.H., RICHARDSON, J.B., III., REITZ, E.J., ROLLINS, H.B., AND MAASCH, K.A., 1996, Geoarchaeological evidence from Peru for a 5000 years B.P. onset of El Niño: Science, v. 273, p. 1531–1533.

SCHROEDER, T., 1993, Climate controls, *in* Sanderson, M., ed., Prevailing Trade Winds: Honolulu, University of Hawaii Press, p. 12–36.

SHERMAN, C.E., FLETCHER, C.H., AND RUBIN, K.H., 1999, Marine and meteoric diagenesis of Pleistocene carbonates from a nearshore submarine terrace, Oahu, Hawaii: Journal of Sedimentary Research, v. 69, p. 1083–1097.

STORLAZZI, C.D., FIELD, M.E., DYKES, J.D., JOKIEL, P.L., AND BROWN, E., 2002, Wave control on reef morphology and coral distribution: Molokai, Hawaii: WAVES 2001 Conference, Proceedings, American Society of Civil Engineers, San Francisco, California, v. 1, p. 784–793.

STORLAZZI, C.D., LOGAN, J.B., AND FIELD, M.E., 2003, Quantitative morphology of a fringing reef from high-resolution laser bathymetry: Southern Molokai, Hawaii: Geologic Society of America, Bulletin v. 115, p. 1344–1355.

STUIVER, M., AND BRAZIUNAS, T.F., 1993, Modelling atmospheric ^{14}C influences and ^{14}C ages of marine samples to 10,000 BC: Radiocarbon, v. 35(1), p. 137–189.

STUIVER, M., AND REIMER, P.J., 1993, Extended ^{14}C database and revised CALIB radiocarbon calibration program: Radiocarbon, v. 35, p. 215–230.

STUIVER, M., REIMER, P.J., BARD, E., BECK, J.W., BURR, G.S., HUGHEN, K.A., KROMER, B., MCCORMAC, F.G., PLICHT, J., AND SPURK, M., 1998, INTCAL98 Radiocarbon age calibration 24,000–0 cal BP: Radiocarbon v. 40, p. 1041–1083.

Received 3 April 2003; accepted 30 July 2003.